AZERBAIJAN REPUBLIC

On the rights of the manuscript

ABSTRACT

of the dissertation for the degree of Doctor of Science

DEVELOPMENT OF NEW MİCRO PİXEL AVALANCHE PHOTODİODES, İNVESTİGATİON THEİR PHYSİCAL PROPERTİES AND APPLİCATİON İN RADİATİON SPECTROMETER

Specialty: 2225.01 - Radiation materials science

Science: Physics

Applicant: **Farid Ibrahim oglu Ahmadov**

Baku-2021

The work was performed at the Institute of Radiation Problems of Azerbaijan National Academy of Sciences.

Scientific consultant:

Doctor of physical and mathematical sciences
Ziraddin Yagub oglu Sadygov

Official opponents:

Correspondent member of ANAS,
Doctor of physical and mathematical sciences,professor
Salima Ibrahim gizi Mehdiyeva
Doctor of physical sciences,professor
Adil Polad oglu Abdullayev
Doctor of physical and mathematical sciences,professor
Rena Jumshud gizi Kasumova
Doctor of physical and mathematical sciences,professor
Musavar Abdusalam oglu Musayev

Dissertation Council BED 1.21 of Supreme Attestation Commission Under the President of the Republic of Azerbaijan operating at the Institute of Radiation Problems

Chairman of the Dissertation Council:

Correspondent member of ANAS
Doctor of physical and mathematical sciences,professor
Oqtay Abil oglu Samedov

Scientific Secretary of the Dissertation Council:

Doctor of philosophy in physics
Muslim Ahmad oglu Mammadov

Chairman of the scientific seminar:

Doctor of physical sciences, associate professor
Matanat Ahmad gizi Mehrabova

GENERAL CHARACTERİSTİCS OF WORK

The actuality of the subject and degree of development. Currently, radiation sources play a key role in the development of nuclear physics, medicine, industry and safety. The determination of energy, type and amount of particles and rays emitted by radioactive sources is extremely important for experiments. Accurate determination of these parameters allows us to correctly define the types, number of new isotopes, the effects than they can produce and the processes inside the nucleus. The high cost of semiconductor based detectors, low temperatures and low radiation resistance create problems for their wide spread use. Therefore, various types of detectors based on scintillator and photodetectorare used widly for this application. In addition, vacuum photomultiplier tubes (PMT), which are used as photodetector, also have disadvantages, such as compactness, high operation voltage, low photon detection efficiency, sensitivity to magnetic fields and vibration make PMT impossible to use in creation of high efficiently and portable radiation spectrometers. At present, semiconductor based photomultipliers - avalanche photodiode (in normal-mode) and micro-pixel avalanche photodiode (in Geiger mode) are widely studied for the improvment of new radiation detectors and spectrometers. Micro-pixel avalanche photodiode (MAPD) are considered to be the optimum one for portable and highly sensitiv scintilation counters and spectrometers. However, MAPD, which is produced by various firms, has a low pixel density and low photon detection efficiency (PDE) and these do not allow them to be widely used. For this purpose, the development of new generation MAPD photodiodes is of great interest to create new radiation detectors.

For this purpose, the study of MAPD's operation mechanism, its physical properties, temperature dependence, radiation dose dependence, and the creation of new ionizing radiation detectors and spectrometers on their basis are topical issues on the present times.

The purpose and objectives of the dissertation:

Theoretical and experimental analysis of physical operation mechanisms of MAPD, improvement of their parameters, the study of the effect of gamma rays, beta particles and neutrons on the signal formation mechanism of these photodiodes and the study of the possibility of using the new generation MAPD photodiode in radiation spectroscopy.

To achieve the aim of this study, the following objectives have been formulated.

• Theoretical and experimental study of the physical working mechanism of MAPD;

• Study of temperature stability of parameters of MAPD;

• Development of methods for improving the parameters of MAPD with surface pixels;

• Investigation of parameters of MAPD with deep buried pixels and their comparison with analogs;

• Study of matrix preparation capabilities based on deep buried-pixel MAPD;

• Investigation of responce of detectors based on various types scintilators and MAPD photodiode on gamma rays, beta particles and neutrons;

• Investigation of sensitivity of detectors based on MAPD photodiodes and scintillator to different energy gamma rays;

• Investigation of pulse shape discrimination performance of detector based on MAPD;

• Studying radiation hardness of MAPD photodiodes;

•Development of electronic parts of MAPD based spectrometer;

• Measurement of spectrometers parameters based on MAPD photodiodes;

Object of study and methods:

The silicon MAPD photodiodes, operated in Heiger mode and spectrometric modules based on them. The properties of the object were studied under various radiation conditions and external influences. The amplitude of the signal received from the devices

was analyzed using the method of mathematical modeling of amplitude distribution and the pulse shape discrimination method were used to define the type of ionizing radiation.

The main scientific provisions include:

1. Improving the stop channel and pixel size for photodiodes allow to develop and test a new avalanche photodiode.
2. Development of a new structure that increases the gain of MAPD photodiodes with surface pixels, photon detection efficiency and reducing the cost of the product.
3. Development of a new iteration model taking into account the resistance of the depletion region for the correct expression of working mechanisms of MAPD photodiodes.
4. Theoretical study of the effect of timing performance of surface pixel MAPD photodiode's over-voltage and parasitic capacitance.
5. Development of voltage convertor and signal amplifier with a bandwidth 45 MHz for radiation detectors and testing them in wide range of temperatures.
6. Development of scintillation detectors based on MAPD-3NK and MAPD-3N1P photodiodes and various types of organic scintillators and identification regularity of energy of gamma ray by the Compton edge
7. Development of new gamma spectrometers based on MAPD-3NK and inorganic scintillators and their comparison with analogues.
8. Study ofthe effect of ≈1.25 MeV gamma radiation on dark currents, breakdown voltage, specific capacity and energy resolution of the MAPD-3NK photodiode.
9. Study of the influence of ≈ 1.25 MeV gamma radiation on the physical properties of the LT-1357 micro-chip operation amplifiers which is used in the detector modules based on MAPD photodiodes.

The scientific innovations resulting from the research are as follows:

- After irradiation with gamma ray (with energy 1.17 MeV-1.33 MeV) up to 250 kGy dose the dark curren of the

MAPD increases linearly in the forward and reverse directions;

- It is shown that the ability of control breakdown voltage of MAPD is possible by changing pixel sizes and concentration, as well as the possibility of reducing the breakdown voltage up to 60 V, it is proposed to increase the concentrationis of the baground region to 3.7×10^{15} / cm^3.
- Development of a new model that accurately illustrates the operation mechanisms of avalanche photodiodes. According to the new model, the gain of SPAD can be twice as high as the actual real value, depending on the resistance of the avalanche channel.
- To decreas the duration of the front edge of the SPAD photodiode, it is necessary to increase the over voltage of the photodiodes, as well as the parasitic capacitance of the photodiodes should be greater than 1% of the pixel capacitance.
- The developed MAPD photodiode's breakdown temperature coficient was 61 mV/ °C for MAPD-3NK, compared to MPPC photodiodes, it was 7% lower than value of MPPC and the photon detection efficency was 5 times higher than MPPC.
- It was found that the dark count of MAPD photodiodes change exponentially depending on temperature, and when the temperature difference is -80 ° C, the dark count has decreased 169 times. Such a decreasing of dark count occurred due to a decrease of generation current.
- A 16 array matrix was designed for MAPD photodiodes. The total area of the matrix was 289 mm^2 (17 mm × 17 mm), and its active area was 219 mm^2. The geometric factor of the new 16-element matrix was 76 %. These matrices are considered optimal sensors for high energy physics and PET.
- It was found that developed detector based on MAPD and p-terphenyl scintillator define energy of gamma rays for Compton edge, and the amplitude of the detector signal

varies linear with energy: ADC = 535.22 + $E_{compton\ edge}$ × 0.31. At the same time, the energy resolution of monoenergetic electrons with energy of approximately 626 keV was 22 %. It has been confirmed that MAPD and perterphenyl scintillatorbased detectors can be used in gamma counters.

- Preparationof a matrix based on MAPD photodiodes, a series combination of elements made it possible to reduce matrix capacitance in accordance to the number of elements in matrix, energy resolution which is equal 20 %. When the MAPD photodiodes are connected in parallel, the matrix capacitance has increased in accordance to the number of elements and the energy resolution is ~ 18 %. The results show that serias combination of MAPD photodiodes is a more efficient in counter mode and flight time application and a parallel combination is suitabel to spectrometric instruments.
- LFS + pterphenyl-based scintillator detectors allow to discriminate gamma rays with energy of 662 keV and mono-energy beta particles with energy of 626 keV in the shape of pulses generated in the scintillator;
- The sensitivity of a scintillation detector based on MAPD-3NK photodiodes and MPPC-S12572-010P photodiodes (manufactured by Hamamatsu) with an LFS scintillator for gamma radiation in the energy range of 26.3 keV-1.33 MeV was investigated. The photodiode MAPD-3NK showed a 34 % better energy resolution for gamma radiation (662 keV) compared to MPPC. This result confirms that the MAPD-3NK photodiode was more optimal for spectroscopic experiments than the MPPC.
- Modeling and preparation of new voltage convertor, amplifiers, discriminators and electronic components for the new designing detector module based on avalanche photodiodes;

- It was proposed to prepare new MAPD photodiodes based on standard CMOS technology. In the proposed new device, in contrast to the surface pixel counterparts, numerous p-n junctions were used as the quenching resistance, which ultimately increased the photon detection efficiency (or quantum efficiency of the photon) of the device. It was proposed to increase the gain with increase the number of p-n junctions;

Theoretical and practical significance of the work:

The first time a new model was developed that accurately describes the avalanche process in MAPD photodiodes. The new model has shown that gain of MAPD varies depending on the resistance of space charge. New proposals were made to improve the parameters of MAPD photodiodes. Based on these assumptions, the gain of MAPD photodiode could be icreased by the voltage which droped on smaller p-n junctions. By increasing the number of p-n junctions, it became possible to increase the over-voltage, the photon detection efficiency and reduce the cost of sample. Effect of pixel radius, background concentration, and antireflection were studied to improve photodiode parameters. Electronic components for MAPD and various scintillation detectors were modeled and prapered. Unlike most analogs, the developed detector module has a linear calibration curve in the energy range of 0.026 MeV-4.44 MeV. The detector responce to beta, alpha particles and neutrons were investigated. The prepared detectors based on MAPD demonstrated a good energy resolution of 34 % to compare with the results obtained with the Japanese Hamamatsu MPPC-S12572-010P photodiode. The matrices based on MAPD photodiodes, their low temperatures, and the influence of energy gamma rays with an energy of 1.24 MeV and 1.33 MeV on the properties of MAPD photodiodes were investigated. Prepared detector modules can be widely used in high-energy physics, space applications, medicine, security, gamma spectroscopy and industry.

Confirmation and approval of the work:

The main results of the dissertation were discussed at international conferences and seminars, such as, “Innovation of scintillation materials and radiation technologies” (2016, Minsk-Belarus), International Workshop on Radiation Visualization Detectors, iWoRID-2016 (2016, Barcelona, Spain), Third International Conference on Radiation and Applications in different fields (2015, Montenegro), International Conference on the Promotion of Silicon Photomultipliers (2018, Switzinger-Germany), 8th international conference “New developments in the field of photodetection” (2017, Tours-France), International Scientific Forum “Nuclear science and technology (2018, Kazakhstan). International Scientific Forum "Nuclear Science and Technology" (2018, Kazakhstan). 12th International ”Hiroshima” Symposium on the Development and Application of Semiconductor Tracking Detectors (2019, Hiroshima-Japan)

Published scientific works:

22 scientific papers were published on the thesis. 15 of these papers were in SAC compliant journals, others were discussed at international conferences and seminars and published as thesis.

The name of the organization in which the dissertation was completed:

The presented dissertation was carried out at the laboratory "Innovative ionizing radiation detectors" of Institute of Radiation Problems of Azerbaijan National Academy of Sciences.

The structure and volume of the dissertation:

The thesis consists ofthe title -1page, content -2 pages (2801 charachters), introduction -8 pages (14531 charachters), chapter 1 - 65 pages (132632 charachters), chapter 2-22 pages (38622 charachters), Chapter 3 -54 pages (87145 charachters), chapter 4 - 43 pages (69979 charachters), chapter 5 -44 pages (66589 charachters), chapter 6 -25 pages (40062 charachters), main results -2 pages (3162 charachters), list of published works on the main results of the dissertation-3 pages (5187 charachters),a list of 200 used references -20 pages (38515 charachters) and a list of abbreviations-3 pages

(2028 charachters). Total page of dissertation is 297 pages, including 196 typing pages, 119 pictures and 3 tables. The total number of symbols in the dissertation are 501253.

MAIN SUMMARY OF DISSERTATION WORK

At the intrudaction, the acctualy of the dissertation work, formulation of objectives and basic tasks, scientific results, practical significance of the case are shown. It also provides a brief overview of the chapters, along with a list of the main provisions for defense, as well as the list of submitted works.

The first chapter provides information on the interaction mechanism of ionizing particles and gamma rays with radiation detectors and parameters that characterize them. One of the main objects of the dissertation research is scintillation detectors based on a photomultiplier and photodiodes and their existing problems. Information about the available analogs of MAPD photodiodes and their parameters. At the end of the chapter, the disadvantages of gamma scintillation detectors based on MAPD photodiodes manufactured by Japan, Germany and Ireland were compared. Noted these detectors were not linearity up to 662 keV. The matris array was suggested to solve this disadvantage, but this approch increased several times of the price of detectors. Other disadvantage of these detectors was bad energy resolution. This disadvantage related directly photon detection efficeny of SiPMs. Finaly MAPDs which will be used in spectroscopy have to have following parameters: high pixel density, high PDE andhigh radiation hardness.

In chapter 2 is described experimental setup which used to measure parameters of MAPD photodiodes: gain factors, quantum efficiency, linearity, dark count, after pulsing, PDE, noise factors, pixel capacitances, operation voltage, dark current, shape of signal and the response of scintillation detectors which is designed based on various scintillators and MAPD photodiodes. Depending on the pulse width of the signal recorded in the experiments, two types of analog digital convertors (ADC) are used. The parameters of the ADC used

were experimentaly determined and their minimal sensitivity areas were obtained. In addition, new voltage convertor with low current (DC), a comparator and a signal amplifier with varios band-width circuit designed and prepared to use detector module.Electronic boards are printed with Protomat S63. The total current requirement of the developed electronic circuit was less than 100 mA. The output voltage of the newly developed voltage convertor was in the range of 90–100 V and fluctation was about ± 0.009 V**.**

The received signal from the MAPD photodiodes is amplified by an amplifier, which is developed on the basis of the LMH6657, LT-1355 operational amplifiers and KT842 transistors. Designed amplifiers have a bandwidth of 30-100 MHz and gains in the range of 10-100. Amplifiers are optimized for reciving signals with a pulse duration from 10 nsec to 500 nsec. The white noise of the amplifiers was 1.8 nA. The voltage converter and amplifier modules were studied to change their properties in the temperature range from +50 ° C to -5 ° C and it was found that these types of modules keept their parameters in a given temperature range. It was found that this type of electronic modules can be used for the production of scintillation detectors.

In chapter 3 Parameters of various types of photodiodes from Zecotek Photonic, Hamamatsu, Laser Companents used in scientific experiments were extensively investigated: Voltage-Ampere Characteristics (Reverse and Forward), Capacitance - Voltage Characteristics, capacitance dependence on frequency,gain dependence on voltage, after pulsing, operating voltage, the distribution of single photoelectrons, the noise figure and breakdown voltage.

Generation mechanizims and disribution of signal with low and high light detection is described in this chapter. Parameters of signal is calculated with Gauss and Puasson distribution.

A new physical model of avalanche process and operation principle with single photon detection capabilities for SPADis presented in this chapter. MAPD from Zecotek Photonics (www.zecotek.com) is fabricated on the basis of a 3 mkm thick

epitaxial silicon layer with *n*-type conductivity has been grown on the surface of a n-typesilicon substrate. An avalanche process takes place betweenn$^+$-p$^+$ rejoin (pixel) in the n-typeepitaxial layer. The active (photosensitive) area of the pixel photodiode is 35 mkm ×35 mkm. The SPAD has following parameters: thickness of depletion region -3 mkm, the breakdown voltage- 42.5 V, capacitance- 0.9 pF, operation voltage- 43-45 V and gain is higher than10^7.

The second MAPD is SPAD-R4523 from Laser Components Company is improving to detect red and NIR part of the spectrum. The SPAD structure consists of p$^+$-π-p$^+$-n+ regions and the avalanche process takes place in the p+ n+ region. The thickness of depletion region, situated between p+ layer and p+ region is about 25 mkm. The diameter of the active area of this photodiode is 500 mkm. SPAD has following parameters: the breakdown voltage-134.6 V, capacitance-1.7 pF, operation voltage- 135-136.5 V and gain is higher than 10^7.

Different type of micropixel avalanche photodiode which had high pixel density was used in this work (from Zecotek Photonics - MAPD-3NK, MAPD-3N1P, MAPD-3D and from Hamamatsu Photonics MPPC-S12572-010P, MPPC-S12572-015C, MPPC-S12572-11-050C). The MPPCs from Hamamatsu Photonics are fabricated on the basis of epitaxial silicon layer with π -type (high purity) conductivity has been grown on the surface of a p-type silicon substrate. Special p^+-n+ regions is created in epitaxial layer and these regions are called pixels. Individual poly silicon micro resistor quenches the avalanche process. Each pixel is covered by additional shielding to reduce crosstalk. π -type high purity epitaxial layer was played key role to decrease number of after pulsing in MPPC.

Depletion region begins from n+-p+ junction when voltage is applied. As increasing voltage thikness of depletion region covers all epitaxial layer and begins increasing electric field in this junction. When applied voltage is equals to the breakdown voltage or higher than it, in this case electrical field changes in $3–5\times10^5$ V/cm region. Electron is accelerated by this field and gets enough energy (3.5 eV) to produce via impact ionization new electron and hole pair in

structure. New created charge is accelerated by field again. This proces will go on and is called avalanche process. This process will continue to infinity if we couldn't control avalanche process in pixel. Indivudial quenching resistor (R_Q) is used to control avalanche process in pixel. The quenching resistor is designed based on TiO material. Each pixel connected throw this resistor to main grid line. Pixels are connected paralel. The output of each pixels summrized and gives main output of MPPC photodiode. MPPC-S12572-010P photodiode has following parameters: pithch - 10 mkm, active area- 3×3 mm^2, number of total pixels- 90000, dark current-20 nA, gain- 100000, capacitance- 320 pF, recover time-20 nsec, PDE- 10 % (470 nm), geometrical factor- 33 %, and operation voltage - 69.5 V. Other MPPC-S12572-015 photodiode has following parameters: pithch -15 mkm, active area- 3×3 mm^2, number of total pixels- 40000, dark current- 20 nA, gain- 230000, capacitance- 320 pF, recovery time- 20 nsec, PDE- 25 % (460 nm), geometrical factor- 53 %, and operation voltage - 69 V. MPPC-S12572-015C and MPPC-S12572-010P areused to obtaine linearity of MAPD, PDE and detect scintillation light from scintillator.Other MPPC-S10362-050CK photodiode is used in experiments. MPPC-S10362-050CK has following parameters: pithch - 50 mkm, active area- 1×1 mm^2, number of total pixels- 400, dark current- 25 nA, capacitance- 38 pF and capacitance of each pixel- 95 fF. Quenching resistor which quenched avalanche proces was defined via forward Volt-amper charachteristic. The current increased as the voltage and the p-n junction was opened in the range of 0.6-1.2 V of applied voltage. Quenching resistor was defined from linear part of curve (due to Om law). Total resistance is obtained as following form $R_{tot} = \Delta U / \Delta I$. If we take a linear part of curve 0.8 V – 1.2 V, then total resistance defined as $R_{tot} = (1.2–0.8) / ((2.091 \times 10^7–5.77 \times 10^5) \times 10^{–9}) =$ 264 Om. Pixels are connected in parallel in this type of photodiodes. The quenching resistance of each pixel is calculated as $R_q = R_{tot} \times N_{pik}$. Thus, $R_q = R_{tot} \times N_{pix} = 264$ Om $\times$ 400 = 105 kOm for each pixel of the MPPC-S10362-050CK photodiode. It is thus possible to

calculate the characteristic time for each pixel $t = R_q \times C_{pik}$ = 105 kOm × 95 fF= 9.975 nsec.

The developed MAPD-3NK photodiodes which used in scintillation detectors have a dark current of 400 nA and an operating voltage of 90.5 V (figure 1). The "E7-20 Измерительиммитанса" device was used to measure the capacitance of the MAPD-3NK photodiode. A sinusoidal signal with amplitude of 40 mV was applied from the E7-20. Such a small amplitude was made to reduce the measurement uncertenties. The amplitude of the sinusoidal signal was much smaller than the voltage droped to the MAPD photodiode. The frequency of the applied signal was 1 kHz, 10 kHz and 1000 kHz. The MAPD-3NK photodiodes have epitaxial layer of the same type. The capacity of the MAPD-3NK photodet was 174 pF (figure 1).

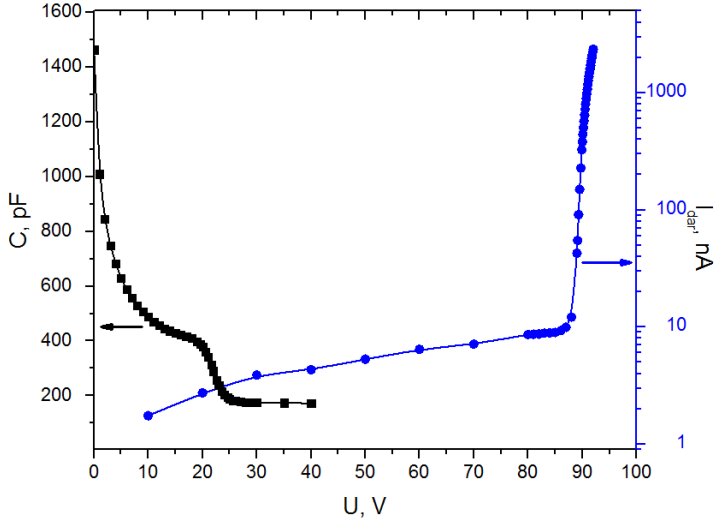

Figure 1. MAPD-3NK Volt–Amper and Volt-Farad charachteristics.

The parameters of the newly developed MAPD-3NK photodiodes were compared to MPPC-S12572-010P photodiodes manufactured by Hamamatsu, Japan (Table 1).

In this chapter also is investigated the quantum efficiency of MAPD-3NK and 3N1P photodiodes (figure 2). The MS3504i monochromator was used to determine the quantum efficiency of MAPD photodiodes. The photocurrent of the MAPD photodiode was measured using Keithley-4867. The voltage applied to the MAPD photodiodes was less than 40 V. This rated voltage was chosen to ensure that the gain does not exceed unity. In this case, the number of created electron-hole pairs does not amplify. To calculate the QE, the etalon PIN- S1223-01 photodiode from Hamamatsu was used. Thelight power from the light source was constant in all measurements. The photocurrent of photodiode has different value depending on the wavelength.

Table 1. Comparison of parameters of MAPD-3NK and MPPC-S12572-010P photodiodes

Parameter	**MAPD-3NK**	**MPPC-S12572-010P**
Geometric Factor (%)	100	33
PDE (450nm)	35-40	8
Pixel density(pix/mm^2)	10000	10000
size(mm^2)	13.69	9
Number of total pixels	136900	90000

Since the sensitivity of PIN photodiodes in the region of 350–1100 nm is known, the QE of MAPD photodiodes was calculated using the following expression:

$$QE_{MAPD} = \frac{İ_{MAPD} \times QE_{PİN}}{İ_{PİN}} \quad (1)$$

Here is the QE_{MAPD}- quantum efficieny of the MAPD photodeode, I_{MAPD}- photo current of MAPD photodiodes, QE_{PIN}- QE of the PIN photodiode and I_{PIN}-the photocurrent of PIN photodiode. The following formula was used to calculate the flux of photons emitted from MS3504i type monochromator on the active area of MAPD photodiodes: F (V / mm^2) = I (A) / (S_{diod} (mm^2) × R (A / V). Where I (A) is photocurrent of the photodiodes generated by light (selected wavelengths), S_{diod}-the area of the illuminated part of the photodiod and R (A / V)- is the sensitivity of photodiode. The photocurrent of the PIN photodiodes was 1051 × 10^{-9} A when monochromator emitted light wavelength of 500 nm. In our case, the illuminated area of the photodiode was chosen 7.065 mm^2 by means of a callibrator. The sensitivity of given PIN photodiode is 4.96 × 10^{-7} W / mm^2 (for wavelength 500 nm), according to datasheet. In the wavelength range of 370–500 nm, the sensitivity of the MAPD-3NK photodiode is 10–47 % higher than that of the MAPD-3N1P photodiod. This difference is directly related to the use of anti-reactive nitride coating on MAPD-3NK photodiodes. The thickness of this layer was chosen so that the minimum reflectance was around the wavelength 450 nm. MAPD-3N1P photodiode sensitivity has increased in the wavelength region of 650 nm - 1100 nm compared to the 3NK photodeode. The quantum efficiency of the MAPD-3N1P photodiode at wavelengths of 900 nm was increased by 2 times compared to the MAPD-3NK photodiode. The increase in quantum efficiency in this region of wavelength is directly related to the fact that the second epitaxial layer of the MAPD-3N1P photodiod is approximately 42 % thicker than the MAPD-3NK photodiod.The obtained results were consistent with theoretically calculated estimates (figure 2).

In addition, the linear region of the MPPC-S12572-010P and MAPD-3NK, 3N1P photodiodes used in the experiments has been investigated and shown that the MPPC-S12572-010P photodiodes in the linear region of 1.5 × 10^5–3.5 × 10^5 photons and linear region of

MAPD-3NK and MAPD-3N1P photodiodes continued up to 1.3 × 10^5 – 5 × 10^5 photon intervals (figure 3). This has shown that detectors based on MAPD-3NK and MAPD-3N1P photodiodes allow detecting high energy gamma rays.

In this chapter was investigated the changing of breakdown voltage, effective capacitance of pixel and dark count of MPPC-S12572-010P and MAPD-3NK photodiodes at low temperatures. The experiments were carried out at the Joint Institue for Nuclear Research in Russia. The pixel density of the used photodiodes was 10,000-15,000 pixels / mm^2. Liquid nitrogen was used in the study

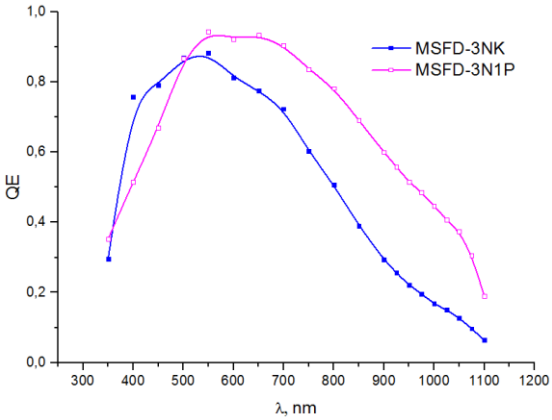

Figure 2. Quantum efficiency dependence of wavelength.

of low temperatures. A pulse generator, CAEN and amplifiers were used to measure the breakdown voltage and single photo electron distribution. The gain of used amplifiers was G1-50 and G2-38. The total gain was 1900. CAEN was triggered by generator during spectral measurments. The temperature dependence of the parameters of the amplifier used at low temperatures was studied for the begining. It was found that the gain of amplifier was changed as following the law G = 504 + 1.28 × T. When the temperature difference was -100 °C, the reduction in the gain was more than

23 %. These changes were taken into account during measurements. This disadvantages was taken in to account all measurements.

LED (450 nm wavelength) was used to determine the gain of the photodiodes and the negative pulse with frequency of 1 kHz, width of 30 nsec and amplitude of 3.34 V were applied to LED. At each temperature, voltage up to 2 V over voltage is applied to photodiode. The breakdown voltage is selected as the point where the line corresponding to the Q-U dependence intersects the stretch line when Q = 0. The gain of the MAPD-3NK photodiodes range 3.3–7.4 × 10^4 in the applied voltage range. To calculate the capacity of each pixel, the dQ / dU ratio was calculated and it was ~ 4.8 × ×10-^{15} F = 4.8 fF for each pixel .Then we examined the change of pixel capacitance values in each temperature range of -38 °C, -73 °C and -108 °C. It was found that the resolution of MAPD-3NK photodiodes significantly decreases with temperature: C_P = 5489 × ×10^{-15} + 2.048 × 10^{-17} × T. Here T is the temperature of the medium (°C). Even when the temperature difference was -80 °C, the capacity change was not more than 34 %. For the MPPC-S12572-010P, the breakdown voltage was 62.4 V. The gain of the MPPC-S12572-010P photodiode changed from 1 to 1.3 × 10^5. The pixel capacity was C_{pik} ~ 3.07 fF. It was found that the capacity of MPPC-S12572-010P photodiodes changed as follows: C_{pik} = 3.885 × 10^{-15} + 1.333 × 10^{-17} × T. When the temperature difference in the MPPC photodiodes was-80 °C , the change in capacity was 31 %.

The temperature dependence ofthe breakdown voltages of MAPD-3NK and MPPC-S12572-010P was investigated. The temperature dependence of the breakdown voltage for the MAPD-3NK and MPPC-S12572-010P photodiodes was found: U_{br} = 86.64 + 0.0616 × T and U_{br} = 64.11 + 0.0654 × T. Here T is the temperature of the external environment. From the results, it was found that the changing of breakdown voltage with the temperature for the MAPD-3NK photodeode was 7 % smaller than for the MPPC-S12572-010P photodiode. In other words, when the same overvoltage is appliedto MAPD photodiodes, their gain decreases with increasing temperature. In this case, the carriers receive more energy (3.6 eV)

between two collisions and the impact ionization occurs. This will allow the brekdown voltage occur at the low voltage region. However, the gain decreases with increasing temperature (at fixed over voltage). This decrease isassociated with an increased probability of carrier energy transfer to optical phonons (reduced average range). To increase the gain , it is necessary to increase the electric field in the region where the avalanche process occurs. This is only possible with increasing voltage. Thatis why the breakdown voltage increases with temperature. The ionization processes also depend on the band gap of the semiconductor. This quantity varies depending on thetemperature. In our case, although the temperature difference was -120 °C, the changing of the bandgap was about 2 %.

Amplitude and dispersion of the photopeak were found using the normal distribution. When the noise factor of MAPD photodiodes measured, the ambient temperature of the photodiodes was -86 °C. The noise factor for MAPD -3NK photodiodes was F ~ 1.04 at the value of 82.7 V – 83.6 V. For other MPPC-S12572-010P photodiodes, the noise factor was F~1,0035 at the value of 66.5 V - 67.5 V. Such a low noise factor made it possible to better separate each photoelectron of the MPPC-S12572-010P photodiodes.

The light-emitting photodiodes were not used when MAPD investigated dark counts of photodiodes. Two amplifiers were used, and CAEN ADC was used to convert the signal. The signal itself was used as a trigger when a signal was detected. It is known that the ratio of the dark count (DC) is mainly due to two types of events: thermal carrier generation in the pn junction of the avalanche region and after pulsing. The concentration of thermal carriers depends on the number of generation centers and the temperature. In addition, DC of MAPD increases as overvoltage. The carriers move from the generation center to the conduction zone and this plays key role to increase DC.That is why measurements were made at different temperatures and different gains. The amplitudes corresponding to the dark photoelectrons were in millivolts. Then, it was investigated that the amount of dark count corresponding to the 5 mV threshold, depending on the temperature, at the same gain. Only the effect of

temperature on the change in DC by the same selection of the coefficient of amplification was studied (figure 4). The temperature dependence of the dark count (DC) corresponding to the 5 mV threshold was determined at the same gain for MAPD-3NK photodiod: $DCR(T)=9{,}44\times10^{8}\times\exp(T/8{,}77)+6{,}045\times10^{5}$. When the temperature difference is -81 °C, DC decreases by about 169 times.The dependence of the dark count corresponding to the first dark photoelectron with the gain is also investigated at the same temperature.When the temperature was -27 °C, the gain increased by 36 % and the DC increase was about 28 %. The increasing the gain caused to increase DC and this changing was associated with an increasing avalanche triggering probabilities of carrier in the MAPD photodiodes. However, when the temperature was -108 °C, the increasing DC of the single-electron was about 75 %. Such changes were observed only at temperatures below -70 °C. This observed change can only be associated with an increased probability of after pulsing pulses. It was also found that the amplitude resolution increases linearly with increasing gain. An increase in voltage also leads to an increase in PDE. For this reason, it is very important to

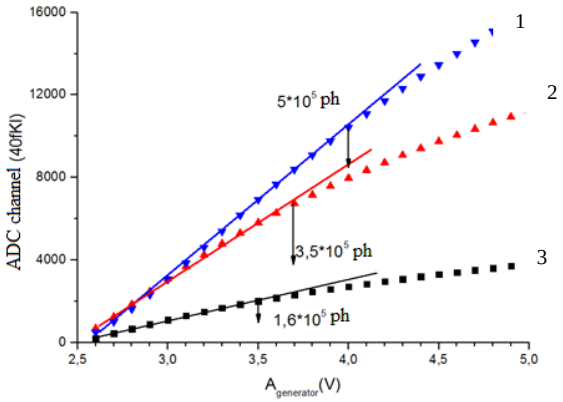

Figure 3. Dependence of the amplitude of the signal with photon number for MAPD-3N1P (curve-1), MPPC-S12572-010 (curve-2) and MAPD-3NK (curve-3) photodiodes.

choose the same gain to investigate the variation in temperature depending on the amplitude. At the same gain, the amplitude resolution of first dark electron was 51 % at -20 °C, 41 % at -67 °C and 35 % at -90 °C. In other words, the amplitude resolution improves with decreasing temperature and when the temperature difference is -70 °C resolution improves to 31 % .

This chapter also was studied the series and parallel combination of elements in preparing arrays matrix based on MAPD photodiodes.

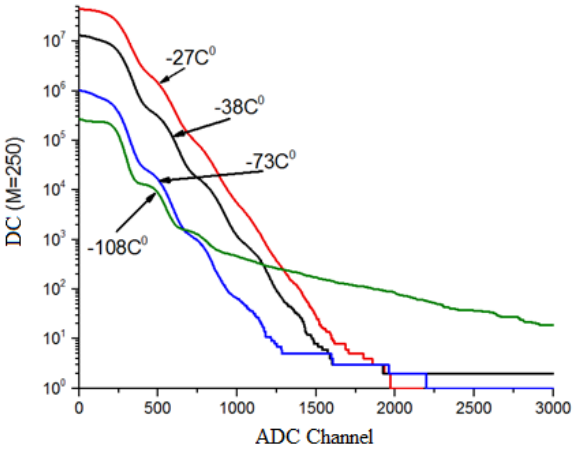

Figure 4. Dependence of dark count with temperature for MAPD-3NK photodiode.

It was found that with a series connection of elements, the matrix capacity decreased to the number of elements and the amplitude resolution was obtained at 20 %. When the MAPD photodiodes are connected in parallel, the matrix capacitance increases to the number of cells, and the amplitude resolution is ~ 18 %. The results of the series and parallel combination of MAPD photodiodes showed that parallel connection of the MAPD photodiodes, a series connection of the MAPD photodiodes is more effective for the preparation of counter and time of flight devices.

Figure 5 shows the CVC of the newly developed MSFD-3NM and previous MSFD-3NK photodiodes. Unlike its previous analogues, the MSFD-3NM photodiodes are full depleted at 20 V. The breakdown voltage of the new MAPD-3NM is ≈ 71.4 V. Theoperating voltage of MSFD-3NM photodiodes range from 74 to 74.8 V. Compared with the MSFD-3NK photodiode, the breakdown voltage of the MSFD-3NM photodiode decreased by ≈ 19 %, the darkcurrent at fixed over voltage (2.6 V) decreased by 5.2 times and theover voltage range increased by ≈ 2 times.

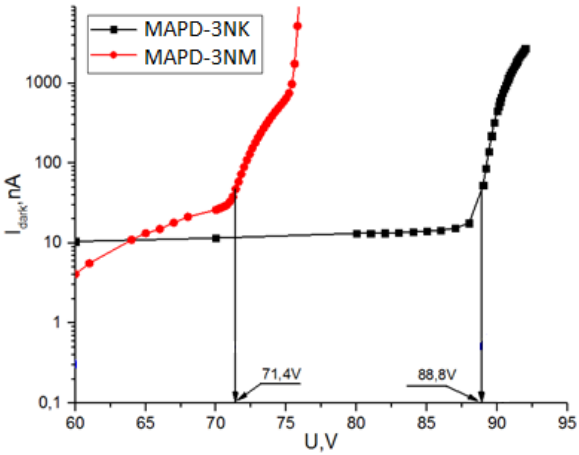

Figure 5. Volt-Amper characteristics of MAPD-3NM və MAPD-3NK photodiodes.

The optimum gain of the MSFD-3NM photodiode was 1×10^5.

In the fourth chapter, a new method and technological process of preparing the stop channel for MAPD photodiodes was proposed (figure 6). In the proposed method, the stop channel is carried out in three stages along the perimeter of the MAPD photodiode. The first stop channel is created on the surface on the substrate. The second stop channel is created over the first epitaxy layer and the third stop channel is created over the second epitaxy layer (figure 6 (a))**.** Then, during the thermal diffusion process, the temperature and annealing

time are chosen so that three stop channels meet with diffusion (figure 6 (b)). In this case, when creating the first and second stop channels, the doseof phosphorus impurity is chosen so that it is less than 10^{14} ions/cm^2, so that the autodoping effect does not occur during the thermal annealing process. The calculations were carried out using the TİDE software package.

For the preparation of the new MAPD photodiode, n-type wafer

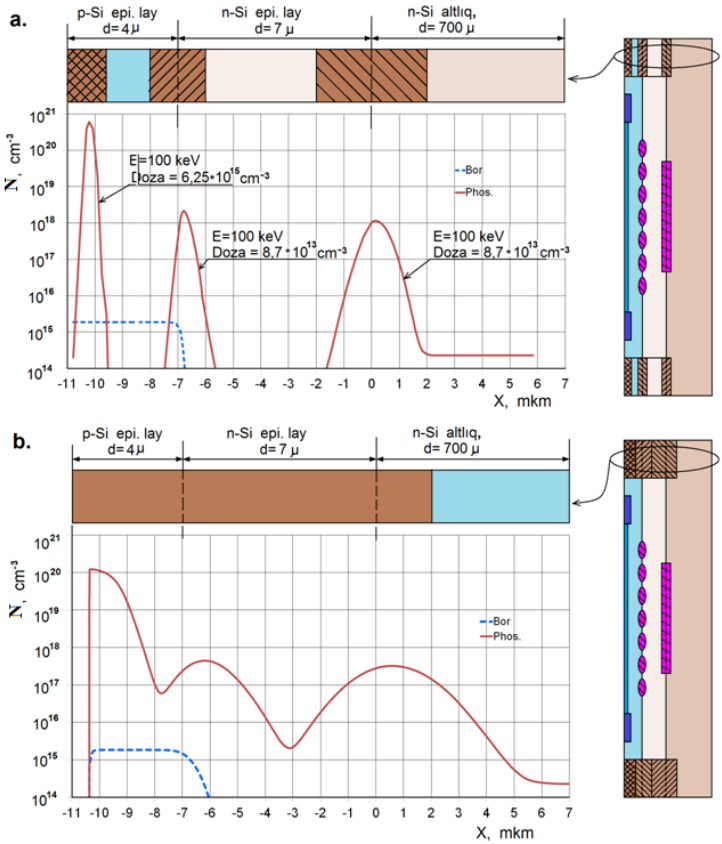

Figure 6. The structure of the stop channel and the distribution of doping (phosphorus ions) in the new photodiode MAPD: a - before thermal annealing, b - after thermal annealing.

with the resistivity of 18 Om × cm and 200 mm in diameter were used (figure 7). Initially, the first external stop channel was implanted using mask-1 on the wafer. At this time, a phosphorus atom with an energy of 100 keV and a dose of 8.7×10^{13} ions/cm^2 was used. Then As ions (arsenium) was implanted to keep electric field in thedepletion volume and for this task is used mask-2. The ion energy waschosen to be 100 keV and the dose was 2.3×10^{13} ions / cm^2. An n-type epitaxial layer (doped by phosphor) with a resistivity of 350 Om×cm and a thickness of 7 mkm was then grown on a wafer. The concentration of n-type in the first epitaxial layer was 1.4×10^{13} ions/cm^3. At the next stage, using a mask-1, phosphorus

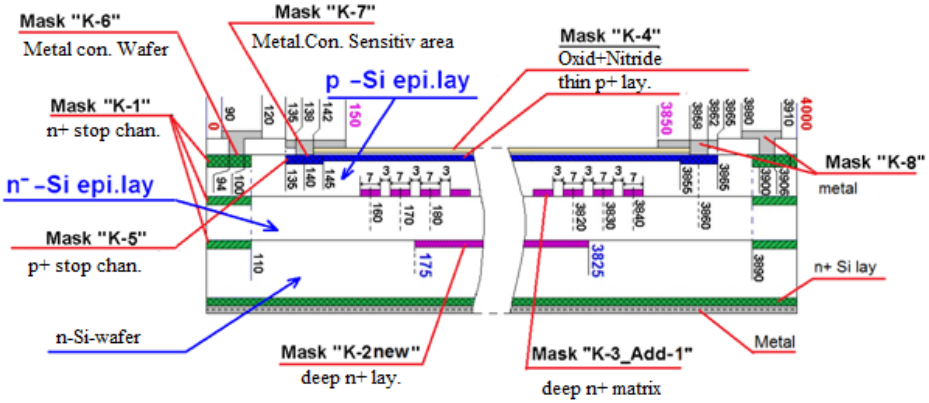

Figure 7. Structure of the newly developed MAPD photodiod.

atom was implanted with an energy of 100 keV with a dose of 8.7×10^{13} ions/cm^2 to form a second stop channel. Then, using the mask-3, the pixel locations were implanted with 100 keV arsenic ion to a dose of 2.3×10^{13} ion/cm^2. The maximum As ion concentration was obtained 3.2×10^{18} ion/cm^3. In this way, a pixel matrix with a diameter of 7 microns and an interval of 3 microns was prepared. Thesecond epitaxial layer of p-type, doped with a boron atom with a resistivity of 7 mkm × cm then was grown the first epitaxial layer. The thickness of the second epitaxial layer was selected 4 mkm.

Then mask-1 is used to grate the second stop channel in this epitaxial layer. The epitaxial layer is implanted with 50 keV of phosphorus ion to a dose of 6.25×10^{15} mkm/cm^2. After implantation of the stop channels, the thermal annealing and temperature were chosen so that at the end of the process, all 3 stop channels were fully combined. Subsequently, the layers of SiO_2 and Si_3N_4 having a thickness of 7 nm and 60 nm were grown along the surface of the photodiode by dry oxidation. Then, the shielding of the electric field and the thin p layer which used as the contact area were prepared with mask-4. For this task, a boron ion with the energy of 40 keV was implanted to at a dose of 3.125×10^{14} ions / cm^2. Then, the stop channel barrier and the contact area of the active site were made using mask 5. For this step, boron atoms with an energy of 50 keV were implanted at a dose of 6.25×10^{15} ions / cm^2. Then, using masks 5 and 6, aluminum was evaporated to the contact zones of the anode and cathode. The thickness of the aluminum layer is 1 cm. The barrier height between the first shielding layer and the wafer was $V_{bi} \sim 0.236$ V. At the same time, the barrier height between this shielding layer and the first epitaxial layer was $V_{bi} \sim 0.31$ V. The presence of such a barrier prevents diffusion of holes into the active region from the wafer. The main purpose of the stop channel is to prevent the diffusion of charge from the sides of the photodiode to the sensitive area ofthe photodiode. In other words, the avalanche process is triggered only by photo signals. In this chapter is investigated the possibility to control the breakdown voltage of MAPD photodiodes by changing the pixel radius and the concentration of the weak doped region.When a pixel has a diameter of 4 mkm and weak doped region concentration is 2×10^{15} cm^{-3} the breakdown voltage is reached of ~ 95 V. When the background concentration was increased up to 4×10^{15} cm^{-3}, the breakdown voltage decreased from 95.5 V to 60 V. This voltage will allow the production of low-voltage MAPD photodiodes in the future. The pixel capacitance of each MAPD-3NK , 3NM photodiodes (1.9 fF), the maximum electric field required for the avalanche process(3×10^5 V / cm), quenching resistor(640 kOm) , the barrier height (0.32 V) and the voltages required to deplete the

first (27 V) and the second epitaxial (12 V) layer were calculated. The results obtained from simulation correspond to the experimental results. In addition, the thickness of the antireflection layer and refractive index of it were determined to increase the quantum efficiency of MAPD photodiodes. It was shown that when a SiO_2 layer is deposited on a Si layer, it absorbs 66.6 % of incident light and 33.4 % of the incident photon reflected from the surface of the structure. For this reason, the quantum efficiency of the MAPD-3A, 3B, 3N, 3N1P photodiodes was obtained 65 %. The refractive index $n_{a.r}$ (450 nm) was calculated as ~ 2.86 for optimal anti-coating and high quantum efficiency. If the layer with a refractive index $n_{a.r}$ (450 nm) ~ 2.86, is grown between the silicon and the SiO_2 layer, about 95 % of the falling photons should be absorbed by the photodiode. In fact, it is impossible to find a material with such a refractive index, since the Si_3N_4 layer is used as a coating material with a similar refractive index. The refractive index of the photon with a wavelength of 450 nm is n_{Si3N4} (450 nm) = 2.1. At the same time, the proportion of photons absorbed in silicon increases sharply. The proportion of photons that absorb silicon ranges from 84 to 97 % and reaches a maximum of 97 %. The thickness of the Si_3N_4 layer varies within 47–85 nm, depending on the wavelength. These results are taken into account in MAPD-3NK and MAPD-3NM to obtain high quantum efficiency at 450 nm, the thickness of the Si_3N_4 layer located between silicon and SiO_2 was chosen as 55 nm.

In this chapter is proposed a new model that correctly explains the avalanche process in single-element avalanche photodiodes (figure 8). The time-dependent of the variation of external and internal currents in single avalanche photodiodes and the effect of the resistance of avalanche channel on the parameters of photodiode are investigated. The new equivalent circuit is taken into account the internal device capacitance C_p, C_q –parasit capasitance, R_s - the resistance of avalanche channel, spark gap and R_p - external quenching resistor (fig.8). The pixel is charged up to U_d voltage through R_q resistance. It is accepted that the parasitic capacity is much smaller than the pixel capacity. Om and Kirchhoff rules was

applied this equivalent circuit and the parameters of the photodiode were calculated. The parameters of photodiode was calculated following forms: the external recharge current: $J = J_{q1} + J_{q2} =$ $= \frac{U_d - U_p}{R_q} + \frac{\int_0^t J_{q2} \times dt}{R_q \times C_q}$, the internal discharge current : $I=qN_i/(\Delta t)$, electric field: $E_i=U_{si}/W$ and the gain: $M = \frac{C_p(U_d - U_{si.min})}{q}$. This calculation was done for simple PIN photodiode.The gain factor for a single electron and a single hole was calculated as $M_e=\exp(\alpha W)$ and $M_h=\exp(\beta W)$ respectively. Here, β are ionization coefficients for electrons and holes and W–the thikness of avalanche region. When the applied voltage is equal or greater than the breakdown voltage, an avalanche process occurs. One photoelectron is created near the anode ($N_{01}=1$) at time $t = 0$. The electron passes through the *i*-layer and creates electron-hole pairs near the cathode. The time this process take is $\tau=(W/v)$, where $v$is drift velocity which is equal to the thermal velocity of charge carriers in the *i*-layer. The number of electrons N_1 collected at the cathode, number of holes P_{02} moving toward the anode, and electric field $E1$ during this step can be expressed as:$N_1= \exp(\alpha_1 W)$, $P_{02}= [\exp(\alpha_1 W)-1]$, $E_1=(U_1/W)$ where $\alpha_1=\alpha(E=E_1)$ and $U_1=U_d$.The holes move towards the anode and create near it new electron-hole pairs after another period of time τ. All these holes are collected at the anode and a new number of electrons N_{02} start the second stage of the avalanche:$_{02}=[\exp(\alpha_1 W)-1]\times [\exp(\beta_1 W)-1]$ where $\beta_1=\beta(E=E_1)$. And so, new electrons appear near the anode after every time period 2τ, starting a new stage of the avalanche. Electric field of avalanche process is expressed as$E=E_2=U_{s2}/W$and different values of the ionization coefficients $\alpha_2=(E=E_2)$ and $\beta_2=\beta(E=E_2)$. As a result, the number of electrons collected at the cathode after the second stage of avalanche process is $N_2=N_{02}\times\exp(\alpha_2 W)=[\exp(\alpha_1 W)-1]\times[\exp(\beta_1 W)-1]\times\exp(\alpha_2 W)$.
Hence, the number of electrons collected at the cathode after the i_{th} stage is $N_i=\prod_{j=2}^{i} \{[\exp(\alpha_{j-1} W)-1]\times[\exp(\beta_{j-1} W)-1]\} \times\exp(\alpha_j W)$ $i\geq 2$ and the electric field at the same time is$E_i=U_{si}/W$. The spark gap voltage will change as following form:

$$U_{si} = U_{s(i-1)} + \frac{U_d - U_{s(i-1)}}{(C_p + C_q) \times R_q} \times 2\tau - \frac{q \times N_{(i-1)} \times R_s}{(C_p + C_q) \times R_q} - \frac{qN_{(i-1)}}{(C_p + C_q)} - R_s \times$$
$$\times \frac{q(N_i - N_{i-1})}{2\tau} \quad (2)$$

The external current across throw R_q is calculated as follow:

$$J_i = \frac{C_p(U_d - U_{s(i-1)})}{(C_p + C_q) \times R_q} - \frac{C_p R_s q N_{(i-1)}}{R_q (C_p + C_q) \Delta t} + \frac{q \times N_{i-1}}{\Delta t} \left(\frac{C_q}{(C_p + C_q)} \right) \quad (3)$$

Where N_i –the number of electrons crated after the *i*-th stage, τ- time of flight in the i-layer,U_d- applied voltage, U_{br}- breakdown voltage, R_p-the quenching resistance and R_s- the resistance of depletion region. The electric field in avalanche region decreases with the number of generated carriers.In order to understand the internal process of avalanche development, it is important to know number of electrons N_i created during each cycle of the avalanche process. Calculations show that the value of N_i rises sharply within a few cycles and reaches its maximum value when applied voltage equals to the breakdown voltage. During the same period, electric potential of the pixel U_p decreases, reaching level of U_{br} at the moment when the number of charge carriers N_i reaches its maximum. These charge carriers leads to further drop of pixel potential well below the breakdown voltage (figure 9a). This changing can be seen from internal current and the pixel voltage dependence on time. The development of the internal discharge current (I) is investigated with time at an overvoltage 1V. The maximum value of the internal current is 0.35 mA that is why some part of voltage drops on the resistor Rs of the depletion region: I × Rs = 0,35 mA×2,3 kOm= 0,8 V. We can see that 0.8V voltage of overvoltage dropped on the resistance of depletion region. The value of the gain dependence on the resistance of the channel is investigated too (figure 9b).

The resistance of the depletion region part is calculated for p^+-n-n structure. When the appliedvoltage equals to the breakdown voltage, the electric field is the maximum at p +n junction. The

current accroses junction can be expressed as: $I = v_s \times \rho \times A$, where ρ is the density of the carriers, A is the area of the p-n junction and v_s – the thermal velocity of carriers (thermal) in p-n junction.The variation of the electric field strength depending on the charge of depletion region (by using the Puasson equation) can be expressed as following $\Delta E(x) = İ \times x/(v_s \times \varepsilon_s \times A)$. Subsequently, the dropped voltage on the depletion region was determined $\Delta U_b = = İ \times x/(v_s \times \varepsilon_s \times A)dx = İ \times W^2/(2v_s \times \varepsilon_s \times A)$. Thus, the following expression is obtained for the resistance of the depletion rgion: $R_s = \Delta U_b/İ = = W^2/(2v_s \times \varepsilon_s \times A)$. Using this expression, the resistance of this part of

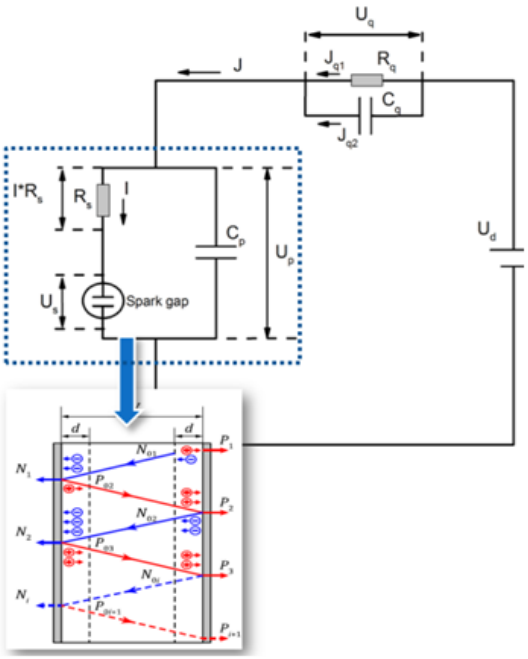

Figure 8. The equivalent circuit of the proposed model.

the depletion layerin the Laser Components' photodiode can be calculated as follows:

$$R_s = \frac{W^2}{2\varepsilon \times \varepsilon_0 \times S_p \times v_s} = \frac{W^2}{2\varepsilon \times \varepsilon_0 \times \frac{\pi \times L^2}{4} \times v_s} =$$

$$= \frac{2}{\varepsilon \times \varepsilon_0 \times \pi \times v_s} \times \left(\frac{W}{L}\right)^2 = 61\text{kOhm} \times \left(\frac{W}{L}\right)^2 \qquad (4)$$

Where W — is thickness of the depletion region, ε_s — dielectric permittivity of silicon, D —diameter of the single-photoelectron multiplication channel, $S_p = (\pi \times D^2)/4$ — area of cross-section of the avalanche channel, $\upsilon_s \approx 10^7$ cm/sec — the maximal thermal drift velocity of charge carriers in silicon.

The new equivalent circuit for single avalanche photodiodes was proposed and proposed model very well matched experimental results (figure 10 a and b). It has been shown that in order to obtain the maximum gain at the same overvoltage, the ratio (W / L) should be smaller than 0.01 (R_s<5 Ω). In other words, low breakdown voltage and low size MAPD photodiodes are considered to be more suitable for the production of high gain photodiodes. In contrast to the similar $C_{pik} \times \Delta Up$ expression for the gain of avalanche photodiodes, the following expression is obtained: $M= m\times C_{pik} \times \Delta U_p = C_{ef} \times \Delta U_p$. Here is the C_{pix}-capacitance of pixel , C_{ef}-effective capacity of the pixel, ΔU_p- dropped overvoltage on pixel and m-constant. The value of m in this expression varies between 1–2 depending on the resistance of the avalanche channel. The volume of m is possible by finding the pixel capacitance (C_{pik}) and at larger capacitance (C_{pik}) value of m decrease and reaches unite. It has also been found that at the same overvoltage, the gain decreases as the resistance of avalanche channel (R_s) increases.

The dependence of timing performance of MAPD photodiodes on the parasitic capacitance has been investigated and it has been established that the front duration of single photoelectron pulse improves to 20 % when the parasitic capacity of the photodiode exceeds 1 % of the pixel capacity.

At the end of this chapter, a new type of MAPD photodiode was proposed. Compared with surface-pixel analog on the developed

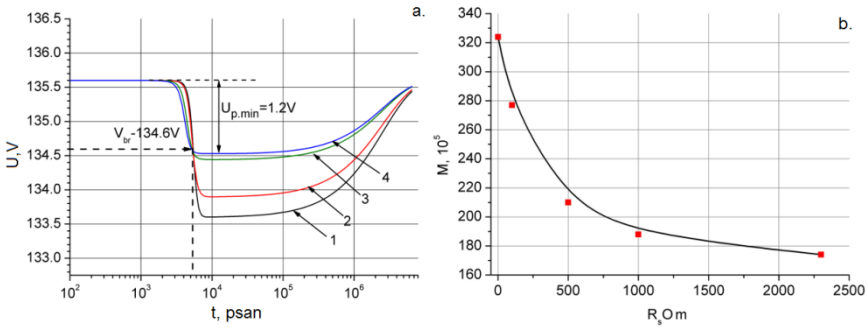

Figure 9. The time depending on the dropped voltage on the pixel of the Laser Component (a) and the value of the gain dependence on the resistance of the channel (b): 1 R_s = 1 Om; 2 R_s = 100 Om; 3 R_s = 1 kOm; 4-R_s = 2.3 kOm.

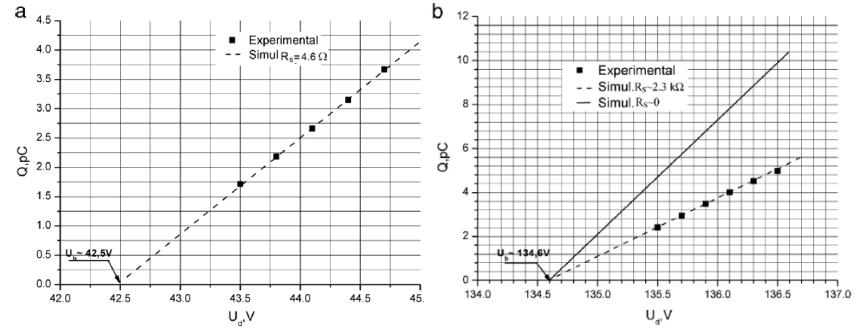

Figure 10. The dependence of the charge on the voltage corresponding to a single photoelectron pulse, recorded by one pixel: a- Zecotek Photonic photodiode, b- Laser Components photodiode.

device was proposed to use small p-n junctions as quenching resistors (figure 11). The use of such small p-n junctions has led to an increase in the geometric factor of the photodiode, resulting in increased device photon detection efficiency. It has been proposed to increase the number of p-n junctions to increase the device's overvoltage and gain. The proposed device consisting of 5 series-connected p-n junctions used as microresistors can operate at an overvoltage of $\Delta V_{ov} = 5 \times 0.7$ V = 3.5 V. This also allows increasing the gain of the proposed device by 5 times according to the prototype. Thus, the gain reaches $M = (2 \times C_{pik} \times \Delta V_{ov}) / q \approx 10^6$, where C_{pik} = 25 fF is the pixel capacity and q- is the electron charge.In addition, the use of serial p-n junction as microresistors for quenching the avalanche process provides a lower cost of the devicecompared to analogs, since the microresistor technology is fully compatible with CMOS technology. Modern CMOS technology allows making p-n junction less than one micrometer in size. Thisallows a pixel interval of up to 1 mkm to be released on the

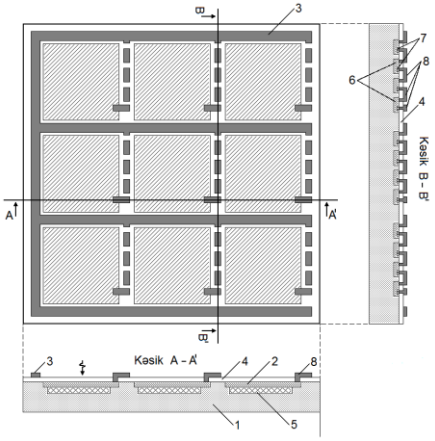

Figure 11 Visualization of the top, side, and cross-section of the avalanche photodiode.

proposed device. This will increase the geometric factor. However, in the known semiconductor photoelectron amplifiers it is not possible to reduce the amorphous sheets microstructure up to 3 mkm, as the thin resistive layer is likely to break. However, the use of p-transitions as a suppressor resistance will allow the parameters of this structure to be more sensitive to temperature. This is intended to allow the device to lower the cost of the device. However, amorphous layers, which are used as micro resistors in known semiconductor photomultipliers, are not able to reduce the layer width to 3 μm, since the probability of destruction of this layer is high. At the same time, the use of p-n junctions as a quenching resistor allows the parameters of this structure to be weakly dependent on temperature.The proposed device is manufactured based on standard CMOS technology, it is expected to decresethe cost of the device.

In the fifth chapter the sensitivity of MPPC-S12572-010P, MAPD-3D and MAPD (3NK and 3N1P) photodiodes in combination with organic (p-terfenyl, fiber scintillator and stilben) and inorganic (LFS and NaI) scintilators to gamma rays, beta particles, alpha particles and neutronshas been investigated.

The used radioisotope sources are point sources available at the Institute of Radiation Problems and their energies range from 32 keV to 3 MeV. During registration of electromagnetic waves of this type, the probability of observing the photopeak is very small and only the efficiency of Compton scattering is high. These detectors allow calculating the energy of gamma rays due to the edge of Compton. The Compton edge of gamma rays emitted by ^{137}Cs and ^{228}Th radioisotopes were observed in channels 600–850. The energy of the Compton edge corresponding to these channels covers the energy range from 473 keV to 2381 keV. The minimum energy of gamma rays detected using this type of detector was 511 keV.

Then, the sensitivity of this detector to other types of ionizing radiation was investigated. For this, the Sr / Y-90 radioisotope was used as a source of beta particles. The Sr / Y-90 radioisotope emits beta particles of various energies the 546 keV and 2284 MeV. The

fact that beta particles have charge and mass made it possible to register this type of radiation. The ^{252}Cf radioisotope was also used to test the effect of neutrons on the detector. The california radioisotope emits fast neutrons in the energy range of 1–5 MeV. This type of neutron was detected as a result of numerous elastic collisions of neutrons with hydrogen compounds of p-terphenyl scintillators. Protons (ionized hydrogen), which receive enough energy from each collision, easily form scintillation photons and these formed photons form a signal. As can be seen from the spectrum of the ^{252}Cf isotope, neutron-related events covered a wider energy region and similar events were also observed in the 1000th channel of the spectrum. These P-terphenyl and fiber detectors are only suitable for detecting ionizing radiation with energies above 511 keV.

The photodiodes MAPD-3N1P and MAPD-3NK with a buried pixel structure were used to detect scintillation photons generated by ionizing radiation. The MAPD-3N1P photodiodes have a pixel density of 15,000 pixels/mm^2, an operating voltage of ~ 95 V, a photon detection efficiency of 30–35 %, an active area of 9 mm^2 and a total number of pixels N = 9 × 15000 = 135000 pixels. MAPD-3NK photodiodes have a pixel density of 10,000 pixels/mm^2, an operating voltage of 90 V, photon detection efficiency of 40–45 %, an active area of ~ 13.7 mm^2 and a total resolution of N = 13.7 × 10000 = 137000 pixels. The size of used p-terphenyl scintillator is 3 × 3 × 35 mm^3. It has been found that detectors based on MAPD and p-terphenyl scintillators discriminate gamma rays by the Compton edge (figure 12), and the amplitude of the signal changes linearly depending on the energy: $ADC=535.22+E_{Com.edge}\times 0.31$. Here is the amplitude of the signal corresponding to the Compton edge and the $E_{Com\ edge}$ - the energy corresponding to the Compton edge and expressed in keVs.

The maximum amplitude of the signal (from ^{137}Cs) detected by MAPD-3N1P and MAPD-3NK was observed on channel 240 and channel 340 of the ADC (figure 13). It is known that during the decay of the ^{137}Cs radioisotope, 93.5 % of the decay proceeds to an energy level of 661.7 keV. However, the emission of 661.7 keV

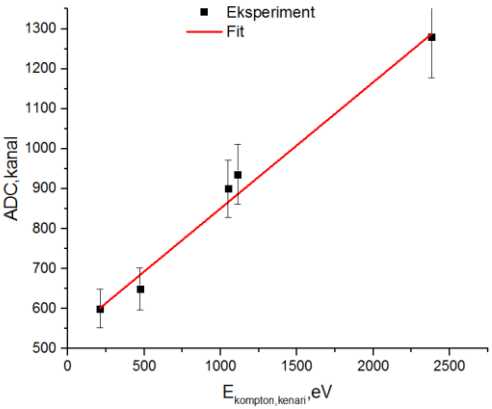

Figure 12. Detector calibration curve based on MAPD photodiode and plastic scintillator.

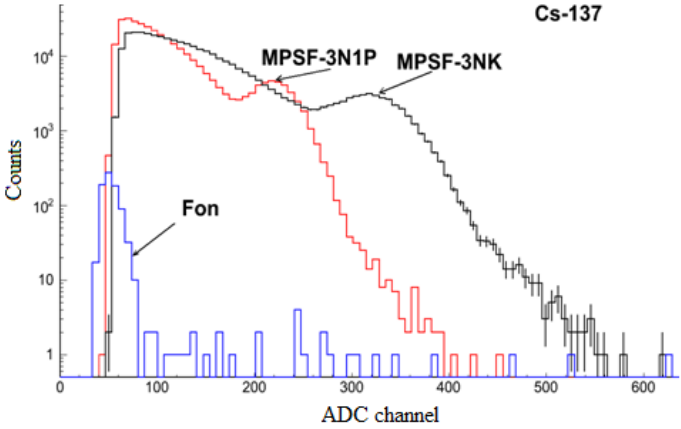

Figure 13. The pulse height spectra of beta particles from ^{137}Cs sources measured with p-terphenyl scintillator coupled to the MAPD-3NK and the MAPD-3N1P.

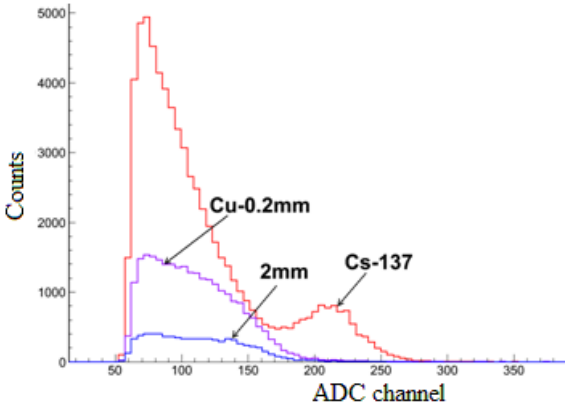

Figure 14 Pulse-height spectrum of gamma rays from ^{137}Cs source is measured with Cu layers.

gamma-ray on this transition is 85.1 %. The remaining 8.4 % is observed for internal transitions. During these internal transitions, the gamma-ray energy of 661.7 keVis absorbed and monoenergetic electron energyof 626 keV is released. In addition, the ^{137}Cs source emits two beta particles with maximum energies of 0.84 MeV and 0.5 MeV. That is why events due to beta particles were observed in the spectrum of gamma rays. Copper layers with thickness 100 and 2000 mkm were placed between the detector and ^{137}Cs sources to check whether events in 186–300 channels of the amplitude distribution spectrum belong to beta particles (figure 14). As can be seen from the spectrum,the number of events associated with beta particles decreased when a 100 mkm thick copper plate was placed between the detector and the radioisotope. When the copper sheets had a thickness of 2 mm, 626 keV beta particles were completely absorbed and only gamma rays with an energy of 662 keV were visible in the spectrum. As the eventsin this section increased with the thickness of the copper sheet, a general decrease in the number of events in the spectrum was observed. The decrease in events in this range is associated with the absorption of the low-energy region of beta particles with a maximum energy of 0.5 MeV and 0.84 MeV. It

was found that the energy resolution of this type of detectors corresponding to a monoenergetic electron with an energy of 626 keV was 22 % (figure 15 a). The performance of fast neutrons detection of stylben based detectors has also been investigated (figure 15 b). It has been shown that MAPD with perterphenyl and stylbene scintillators can be used for the preparation of gamma and

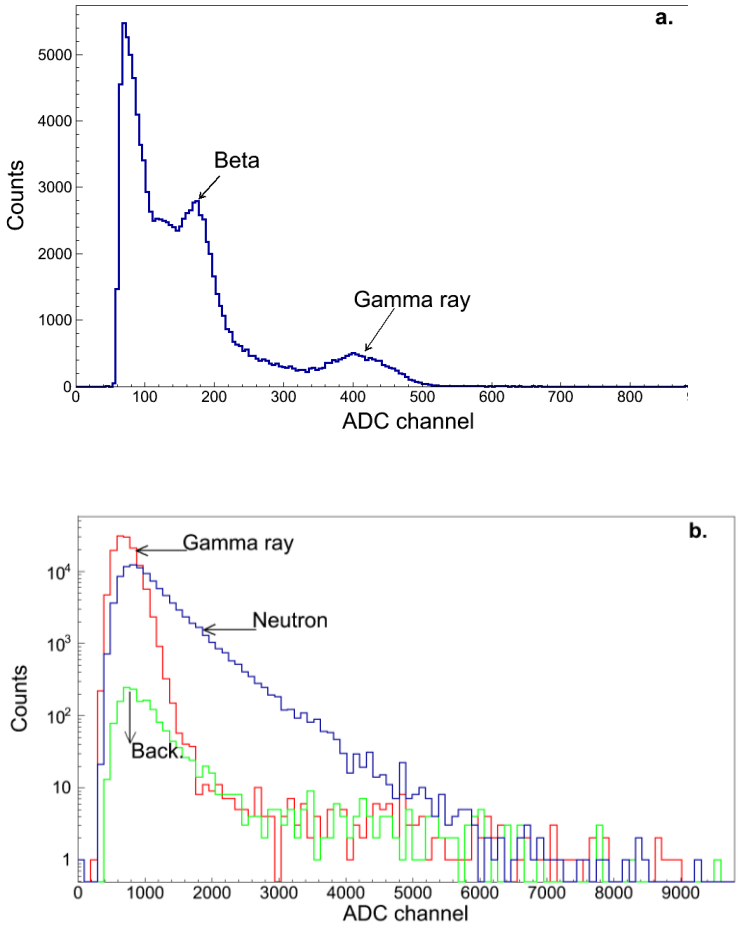

Figure 15. Amplitude distribution spectra of beta particles, fast neutrons, and gamma rays detected by the P-terphenyl and stilbene scintillator and the MAPD-3N1P photodiode.

neutron counters. However, these types of detectors are not suitable for spectrometric measurements.

Then gamma rays were recorded using an inorganic scintillator LFS-3. The used LFS scintillator has the following parameters: density was 7.35 g/cm^3, the maximum radiation wavelength was 416 nm, the decay time was 36 nsec and the photon yield was 80–85 % (NaI). The size of the LFS-3 crystal was 3 × 3 mm^3.

The parameters of the MAPD-3N1P photodiodes used in the experiment were as follows: operating voltage - 94.5 V, dark current - 120 nA, gain - 6 × 10^4 and PDE -30 %. The G-36 amplifier was usedto amplify the signal received from the MAPD photodiode. Radioisotopes with an energy of 26.3 keV - 1.33 MeV were used as a source of ionizing radiation. Figure 16 shows the amplitude spectrum of 59.6 keV gamma ray which detected by scintillation detectors basedon MAPD-3N1P and LFS-3. Since the surface of the scintillator is covered with several thin layers, the probability of alpha particles entering the scintillator is impossible in this case.The maximumsare observed in two photopeaks on channels 740 and 2012 of ADC. The thickness of the copper plate needed to completely absorb the gamma ray of 26.3 keV (channel 740) was determined using a simulation program. When a 1 mm thick copper plate was placed between the ^{241}Am radioisotope and the detector, it was observed that the 26.3 keV energy was absorbed fully in this layer. The maximum of the photopeaks observed in the channel in 2012 which belongs to 59.6 keV and energy resolution was 35 %. The gamma ray spectrum of the ^{133} Ba radioisotope (figure 17) was then detected using LFS and MAPD-3N1P photodiodes. A maximum of 5 photopeaks can be observed in the amplitude distribution spectrum: channel 921, channel 2644, 5692, 10552 and 12557.The peaks in the spectrum fall on channel 921 correspond to energy of 31 keV, a channel 2644 incident for an 81 keV energy gamma ray, an event of channel 5692 due to multiple scattering of gamma rays, events on channel 10 553 correspond to energy of 303 keV and the event on channel 12557 correspond to energy of 356 keV. These dates for the ^{133} Ba radioisotope are fully consistent with literary dates.

The gamma-ray spectrum of the ^{137}Cs (662 keV) radioisotope which used widely in the many experiments is shown in figure 18. The spectrum shows a 662 keV photopeak, Compton edge, scattering and X-ray (32-keV) characteristic for the K level of the ^{133}Ba isotope. As can be seen from the spectrum, the 1700th part of the ADC channel corresponds to the Compton edge and the 23265th part corresponds to the photopeak of 662 keV. A Gaussian distribution was used to find the photopeak parameters in the spectrum. The standard deviation of the photopeak corresponds to σ ~ 1074.8 channels.

The energy resolution corresponding to the photopeak was

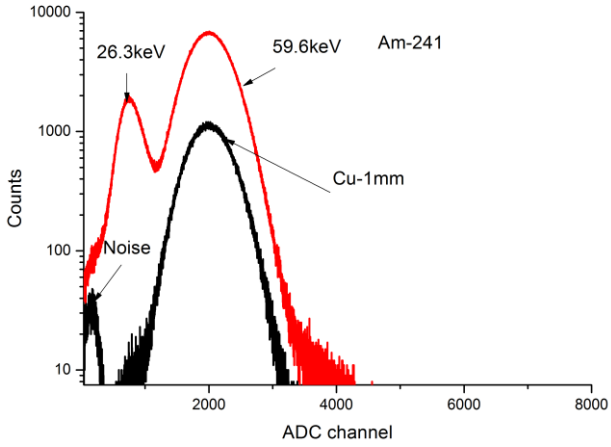

Figure 1 6. Pulse-height spectrum of gamma rays from ^{241}Am (left) source is measured with LFS scintillator coupled to MAPD.

calculated using as following formula $R = 2.35 \times \sigma / Xc$. Where σis the standard despertion of the photopeak and Xc- photo is the maximum of photopeak. The obtained energy resolution for gamma

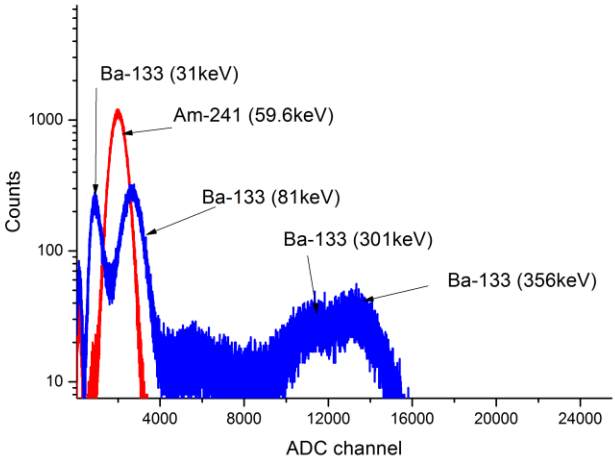

Figure 16. Pulse-height spectrum of gamma rays from ^{133}Ba,^{241}Am and ^{22}Na sources are measured with LFS scintillator coupled to MAPD

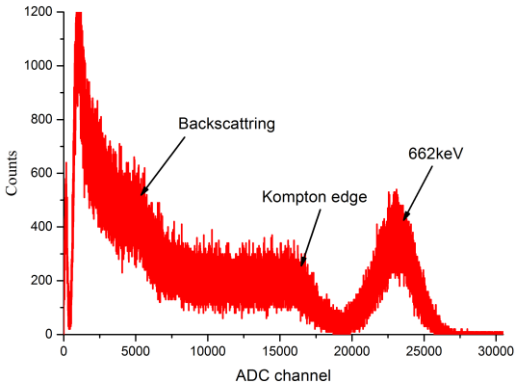

Figure 18. Pulse-height spectrum of gamma rays from ^{137}Cs source is measured with LFS scintillator coupled to MAPD

radiation of 662 keV is R ~11.2 % using “MAPD+LFS” scintillation detector.

Figure 19 shows the distribution spectrum of gamma rays with higher energy. As can be seen from the spectrum, the positionsof the photopeak's maxima corresponding to the energy gamma ray of 1.17 MeV and 1.33 MeV can be observed and these peaks were observed in the channels 23181 and 26710 of the spectrum. Althoughthe amplitude of the photopeak from the spectrum has been obtained, other parameters cannot be calculated. This disadvantage isdue to the small size of the scintillator.

Thus, the energy dependence of the photopeak amplitudes of gamma rays in the energy range 26.3 keV - 1.33 MeV was invetigated by the scintillation detector based on the LFS and MAPD photodiode (figure 20). The error was 5 %. MAPD-3NK photodiodes with inorganic (LFS) scintillator detectors can discriminate ionizing gamma rays by photopeak and amplitude increases as increasing energy of gamma-ray -ADC (channel) = -180+ 35.9 × E (keV).

Further investigated the performance of gamma-ray detection of the newly developed MAPD-3NK photodiodes and MPPC-S12572-010P photodiodes manufactured by Hamamatsu. The calibration curve of both photodiodes is fully linear in the energy range of 26.3 keV–1.27 MeV. It should be noted that for a 662 keV gamma-ray, a detector based on MAPD-3NK photodiodes demonstrated 13 % of the minimum energy resolution. The MAPD-3NK photodiodes have 34 % lower resolution than the MPPC-S12572-010P (figure 21). At the same time, the minimum energy detected by MPPC-S12572-010P photodiodes were 59.6 keV, for MAPD-3NK it was 26.3 keV. From the results, it was found that MAPD-3NK photodiodes are more suitable for spectroscopic experiments than MPPC-S12572-010P. At the end of this chapter was investigated gamma and beta particle discrimination of detector due to the pulse shape. For this purpose, the ^{137}Cs radioisotope was used. In practice, the ^{137}Cs source is used for this purpose. It emits gamma rays with an energy of 662 keV and beta particles with a

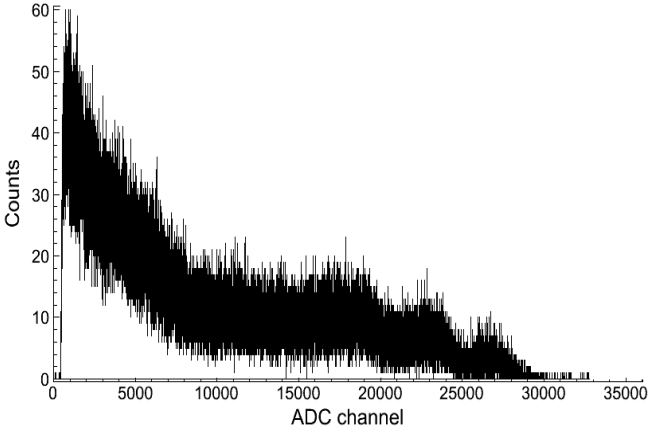

Figure 19. Pulse-height spectrum of gamma rays from ^{60}Co source is measured with LFS scintillator coupled to MAPD (attun. 1.8)

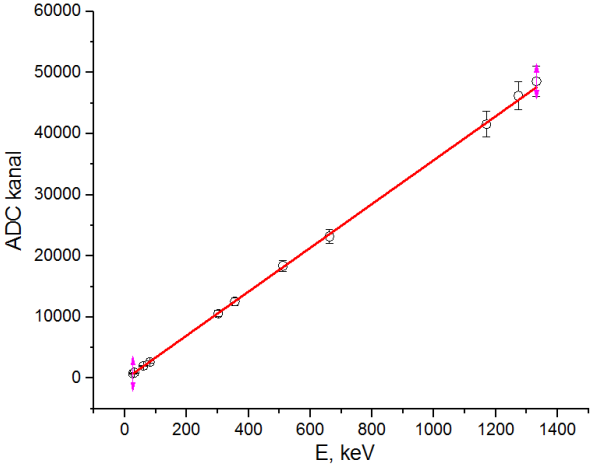

Figure 20. The calibration curve of the LFS+MAPD detector in the gamma energy range from 26,3 keV to 1,33 MeV.

monoenergy of 626 keV.The energy resolutions of 662 keV gamma ray detected by the LFS was 15 %. From the distribution of amplitudes it was found that the amplitudes corresponding to the photopeak of gamma radiation and monoenergetic beta particles differ 2.1 times. But in fact, the difference of the energy of gamma rays and monoenergetic electrons is about 6 %. Although the energy of ionizing radiation is close, the sharp difference is related the light output of the scintillator (p-terphenyl and LFS-3) and the PDE of MPAD for the light wavelength emitted from scintillators. A special algorithm was used to descriminate which of the events detected in the prepared detector belonged to gamma and beta particles.

The main goal is to discriminate the scintillator events due to decaytime of scintillators. Initially, the digital signals are normalized,

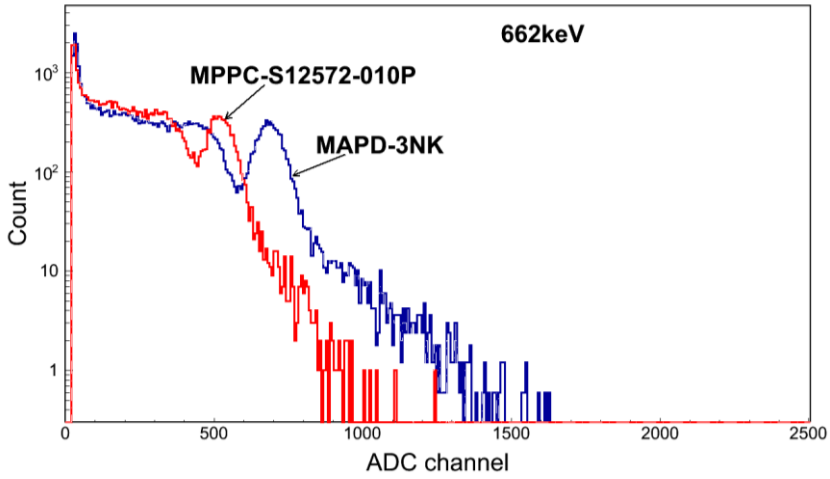

Figure 21. ^{137}Cs radioisotope spectrum detected with MAPD-3N1P and MPPC-S12572-010P photodiodes

the maximum is found, and the integration gate on the rising and falling is selected 120 channels. Signals with a small pulse width are located in one spectrum and signals with a pulse duration long in another spectrum. It was found that the newly developed phosphich

detector can be discriminated by beta particles and gamma rays in the shape of the pulse.

In sixth chapter discussed the development of sensitive gamma spectrometers based on MAPD photodiodes and their study of radiation hardness. Detailed information was given about the elements of the developed spectrometric module, their working principle and parameters.

Figure 22 shows the electronic circuit of the gamma spectrometer. 1-DC-DC voltage circuit provides high voltage source for MAPD photodiodes, 2-voltage inverter provides negative voltage source for circuit, 3-amplifier amplifies out put signal of MAPD, 4-comparator provides to detect siganal which has higher amplitude than threshold, ADC- converts analog signal to digital signal and 6- personal computer implements processing and storage of converted digital signals.The event corresponding to each channel of

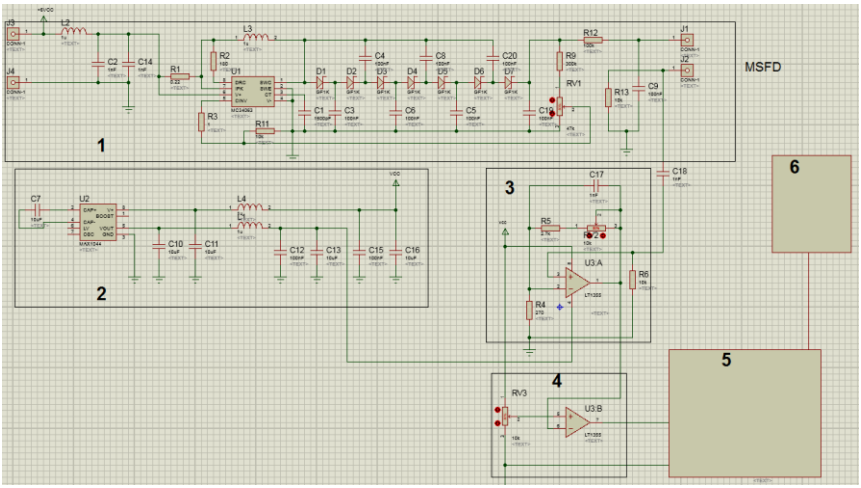

Figure 22. Electronic circuit of gamma spectrometer 1-DC-DC voltage converter, 2-voltage inverter (voltage source), 3-signal amplifier, 4-comparatorr, 5-ADC MCA analyzer and 6-PC.

the spectrometer is 0.12 mV different from the other. This valueis considered the minimum recorded amplitude. The charge corresponding to each channel of the ADC is $I = 1.2\times10^{-4}$ V/ 50Om= $= 0.024 \times 10^{-4} = 2.4 \times 10^{-6}$ A, where the charge for each channel is calculated $q = I \times t = 2.4. \times 10^{-6}$ A / $5 \times 10^{9} = 0.48 \times 10^{-15}$ C. The charge of each channel of the spectrometer was 0.48×10^{-15} C. MAPD-3NK photodiodes and NaI (LFS) scintillator was used during spectrometer preparation. The spectrum converted by ADC was analyzed on the computer using algorithms that were written in C ++.

Figure 23 shows the recorded spectrum of the distribution of the amplitudes of gamma rays emitted by the PuBe radioisotope with thenew SPECTRIG MAPD module. As can be seen from the spectrum, the newly developed spectrometer is linear up to 4.44 MeV.

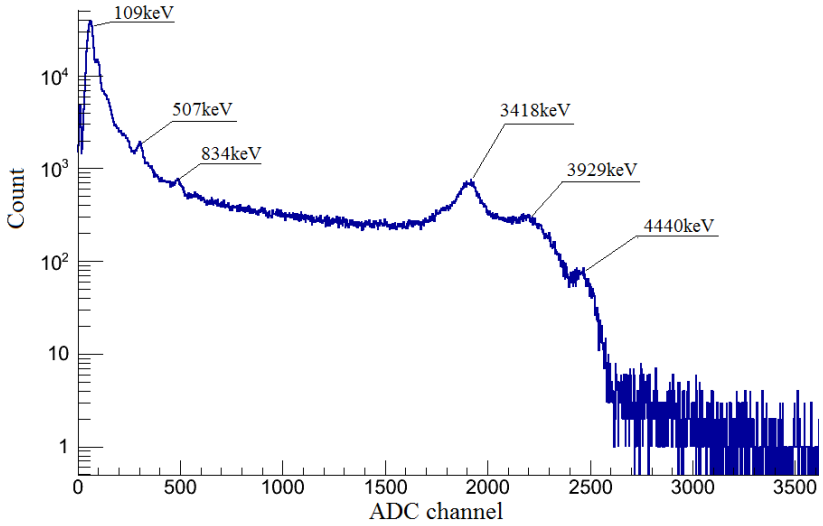

Figure 23. PuBeradioisotope spectrum detected with SPECTRİG MAPD and Naİ

In this chapter also was investigated the radiation hardness of MAPD-3NK photodiodes at 250 kGy and amplifier at 610 kGy dose.

After irradiation, the dark current of MAPD-3NK photodiodes increased approximately 15 times. Figure 24 shows the dependence of dark current at the operating voltage of the MAPD photodiodes (90.5 V) on the gamma radiation dose. As the dependence doses increase, the dark current of MAPD photodiodes increases, which is the line of growth: $I_{da} = 938.7 + 51.6 \times D$. Here I_d is the dark current (nA) and D- radiation dose (kGy) at the operating voltage of the photodeode.

The increasing of the total dark current of the irradiated photodiode was due to an increase in the generating current in the depletion region. The generation centers is generated by electrons which was genarated gamma rays with energies of 1.17 MeV and 1.33 MeV. New created electrons give enough energy (up to 15 eV) to the Si atoms in the lattice to cause them to leave the lattice position. Exactly these defects create new generation and other types of capture (retention and recombination) centers. Since the gamma ray can completely penetrate the MAPD photodide, the effects created by it are evenly distributed throughout the volume. These generation centers occur in epitaxial layers, which are the active volume of the MAPD photodiod. The concentration of these generating centers increases linearly as the dose of radiation increases. The current of MAPD photodiodes measured by the Keithley-4867 device equals to sum of the surface current (which does not participate in the amplification) and the avalanche current and is expressed as follows: $I = I_{sur} + M \times \dot{I}_{gen}$ here J_{sur}- the surface current , J_{gen}- generating current (involved in amplification) and M-gain of avalanche process. As can be seen from the expression, the total MAPD current increases with increasing generation current and both of them increase linearity with increasing radiation dose.

Figure 25 shows the dependence of the differential current $\Delta\dot{I}=(\dot{I}_n-\dot{I}_{n-1})$ on the differential voltage $\Delta U=(U_n-U_{n-1})$ of irradiated photodiodes with gamma radiation. The parameters were measured with a Keithley-6487 picommeter. The differential dependence was considered in the voltage region, where the dark currents gradually changed. For MAPD photodiodes, this voltage region is maintained

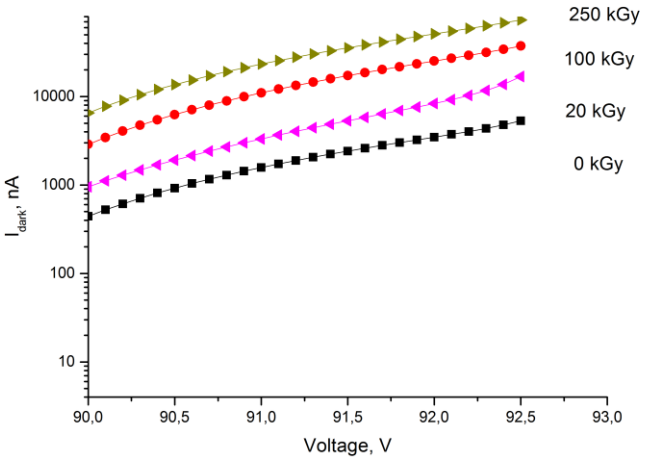

Figure 24. Dependence of the dark current of the micro-pixel photodiode at different doses of voltage

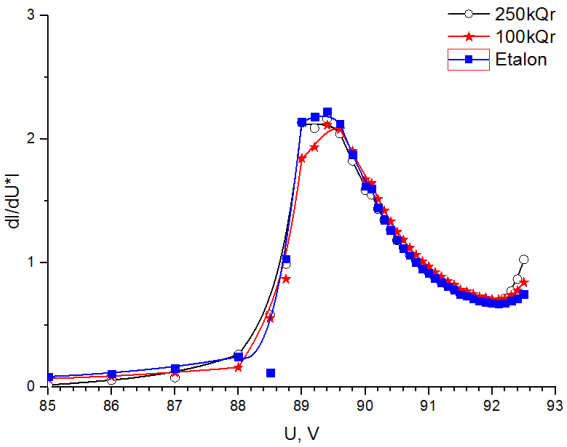

Figure. 25. The dependence of the ratio of the differential voltage - dark current of the micropixel avalanche photodiode at different doses

at a higher voltage, starting from 88 V. At a voltage of 88-89 V, the rate of the dark current increases sharply. This event was associated with the avalanche process occurring in p-n junction. The voltage value in the subsequent voltage of 89-89.6 V corresponds to the breakdown voltage in most cases, and the voltage corresponds to the value of 89.3 V for all three photodiodes. The avalanche process is quenched by the quenching resistance (with further voltage) and the rate of the dark current slows down. Therate of the differential current in the voltage range of 91.6–92.3 V rapidly decreased and approached saturation. This case is considered the most optimal. In this case, gain , PDE and energy resolution are optimal. For this reason, this area is called the operating voltage. At further voltages, rate of the differential current increases dramaticly. This change is associated with the formation of uncontrolled avalanche process in the structure of the photodiode. Thus, after a radiation dose of 250 kGy, significant changes in the breakdown andoperating voltage of MAPD were not observed. No significant changes in the capacitance of the irradiated MAPD-3NK photodiodes were observed. The results showed that detectors based on MAPD-3NK photodiodes can be successfully used in conditions of strong gamma radiation for a long time. This will increase the life of gamma spectrometers and dosimeters.

In this chapter was investigated the dependence of signal amplifier properties on radiation dose based on LT-1357 operating amplifiers. The gain of the LT-1357 was 10 and its bandwidth was 2.5 MHz. The parameters of output signal of the amplifier based on the LT-1357 were measured by the Hantek DSO-5202 oscillascope. Four amplifiers based on the LT-1357 with a gain G ~ 10 were used durning this measurments. The amplifiers were irradiated with gamma ray with E > 1 MeV energy emitted from ^{60}Co radioisotope at 4 doses: 20 kGy, 250 kGy, 400 kGy, 610 kGy. Parameters that characterize the amplifiers was investigated after each irradiation phase: gain, current and bandwidth. There were no significant changes in the bandwidth of the amplifier and the gain of the doses of the irradiating radiation at a value of 20 kGy - 250 kGy. The

amplifier bandwidth covers 0–586 kHz intervals (figure 26). The amplifier bandwidth was 0–484 kHz at a radiation dose of 400 kGy. The bandwidth of the amplifiers decreased by 17 % after irradiation. The bandwith of amplifier was observed at a frequency of 442 kHz, when a radiation dose was 610 kGy. In this case, the bandwidth of irradiated amplifiers decreased by 24.5 % compared with the initial case. The dependence of the amplifier gain on the doses was studied. It was found that after 400 kGy irradiation dose the amplitude of sinusoidal signal (amplitude -100 mV and a frequency - 10 kHz) decreased 0.8 %, but at a dose of 610 kGy the reduction was up to 4 %.

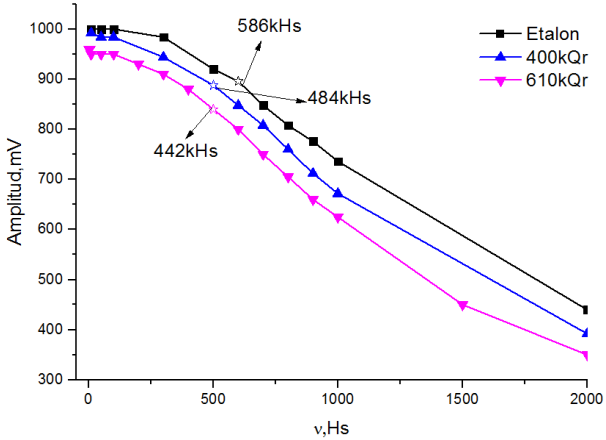

Figure 26. Dependence of the band width of the amplifier at different doses.

It was also investigated that the current requirement for an amplifier depends on the radiation dose (figure 27). The amplitude of the signal from the generator varied in the range from 20 mV to 320 mV. At this time, the current requirements of the reference amplifier increased from 2.51 mA to 11.36 mA. At an irradiation dose of 400 kGy, the current requirement ranged from 2.16 mA to 10.77 mA. At an irradiation dose of 610 kGy, the current requirements ranged from 1.76 to 10.25 mA. Apparently, with an

increase in the radiation dose, the current requirement of the amplifier decreases. The current requirements for amplifier (an amplitude of 100 mV and frequency of 70 kHz) before irradiatio for referenc amplifiers were 4.76 mA. After irradiation dose of 400 kGy, the current consumption of the amplifier was 4.35mV and decreased by ~ 8.6 %. At a radiation dose of 610 kGy, the requirement for the amplifier current was 3.91 mA thus, the requirement for the amplifier

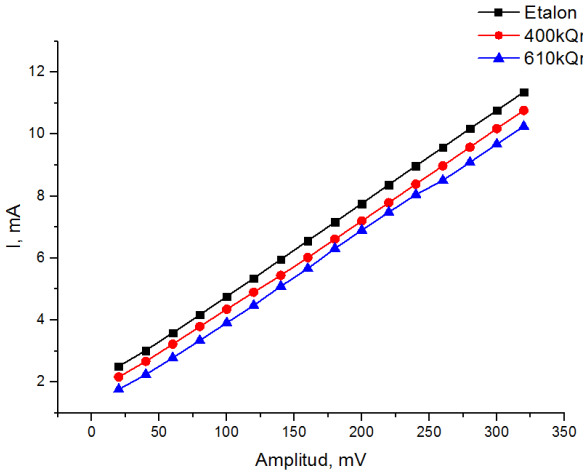

Figure 27. Dependence of the amplifiers current on the amplitude at different irradiation doses

current was reduced by ~ 17 %. Despite the high dose properties of the signal amplifiers, these can be successfully used on spectrometers based on NaI and CsI scintillators.

RESULTS

The scientific findings and main results obtained in the dissertation are summarized in 9 paragraphs:

1. Anew deep-buried MAPD photodiode with improvedtheir guard ring stop-channel and pixel sizeare developed and tested. In comparison with MAPD-3NK, the new MAPD-3NM type photodetectors have a 19% low operating voltage, 5.2 times less dark current and 80% more avalanche gain.. It was obtained that the photodetection efficiency of new developed MAPD photodiode is 5 times higher than analogue.

2. A new structure of MAPD has been developed to improve photodiodes parameters, increase gain, photodetection efficiency and reduce cost. The proposed device uses a series of micro p-n junctions as quenching resistors. It has been found that the new MAPD photodiodes can exceed their analogs by 50 % in terms of performance.

3. A new iterative model has been developed to accurately describe the mechanism of operation of MAPD type photodiodes, taking into account the resistance of the depletion region. It has been found that the gain of MAPD type photodiodes can be doubled depending on the resistance of the depletion region.

4. It was found that rising time of the MAPD photodiodes can be got with increasing the overvoltage to 4 V and the parasitic capacity to 1 % of the pixel.

5.A signal amplifier with 45 MHz bandwidth and voltage converter with 9 mV fluctation has been developed and tested for radiation detectors based on MAPD-type photodiodes. It has been found that the electronic components retain their parameters in the temperature range +50 ° C - -5 ° C.

6.The radiation detector based on MSFD-3NK and MSFD-3N1P photodiodes and various types of organic scintillators have been developed and been extensively studied. It was shown that detectors based on MAPD and p-terphenyl scintillators can discriminate gamma rays for the Compton edge, and the signal amplitude of this

detector changes linearly with energy i.e., ADC = 535.22 + $0.31 \times E_{Com.edg.}$.

7. A new gamma spectrometer has been developed based on MAPD-3NK and inorganic scintillator. It was found that when registering gamma radiation energy of 26.3 keV - 1.33 MeV, this detector exceeds its analogue by 34 % in energy resolution and these detectors are linear up to 4.44 MeV.

8. The effect of gamma radiation with an energy of ≈ 1.25 MeV on the dark current, breakdown voltage, capacitance, and energy resolution was studied. It was found that after irradiation a dark current, the energy resolution increased by 15 times and energy resolution by 8.7 %, the capacitance and breakdown voltage remained constant with an accuracy of 5 %.

9. The influence of gamma ray with energy of ≈ 1.25 MeV on the physical properties of LT-1357 micro-chip amplifiers used in MAPD photodiodes based detector modules were studied. The amplifier is irradiated up to 610 kGy. It was found that after 610 kGy of irradiation dose, the amplifier gain and bandwidth decreased by 4 % and 24.5 %, but the current consumption improved by 17 %

List of Publication

1. Əhmədov F., Mikro pikselli selvari fotodiolar və p-terfenil əsasli radiasiya detektorlari // Milli Aviasiya Akademiyasının Elmi Əsərləri, Cild 21(3) , 2019. s,37-43.
2. Sadıqov Z.Y., Yarımkeçirici fotoelektron gücləndirici/ Əhmədov F.İ, Əhmədov Q.S., Sadıqov A.Z., Süleymanov .S.S, (patent) Sənədin nömrəsi a 2016 0057, Bakı – 2019,№ 5 , s.15.
3. Ahmadov. F, Investigation of silicon photomultiplier at low temperature// Azerbaijan Journal of Physics, -2019, vol. XXV, Number 03, -p.15-19.
4. Əhmədov F., Selvari fotodiodlarin radiasiya davamliğinin öyrənilməsi// Azerbaijan Journal of Physics, -2019 vol. XXV, Number 03, , -s.7-12.
5. Əhmədov F., Silisium əsasli fotoelektron gücləndiricilər // Gənc tədqiqatçı, -2019, Cild 5, №2, -s.5-16.
6. Əhmədov F., Mikro pikselli selvari fotodiodlar əsasinda radiasiya detektorlarinin hazirlanmasi // Gənc tədqiqatçı, -2019, Cild 5, №2,- s.33-43.
7. Ahmadov F., Development of compact radiation detectors based on MAPD photodiodes with Lutetium Fine Silicate and Stilbene scintillators/ Ahmadov G., Garibov A., Guliyev E., Khorev S., Sadigov A., Sadygov Z., Suleymanov S.,// Journal of Instrumentation,- 2015, Vol.10,- p.1-7.
8. Sadygov Z., A new method to improve multiplication factor in micro-pixel avalanche photodiodes with high pixel density/ Ahmadov F., Ahmadov G., Sadigov A., Suleymanov S., Madatov R. // Nuclear Instruments and Methods in Physics Research Section, -2016, Vol. 824, -p.137–138.
9. Ahmadov F., Investigation of disadvantagesof LFS scintillator/ Sadygov Z., Jafarova E., Madatov R., Ahmadov G, Sadigov A., Suleymanov S.,// ANAS. Journal of Physics, -2016, Vol. XXXVI, Number 5, -p. 20-22.
10. Ahmadov F., New gamma detector modules based on micropixel avalanche photodiode/ Ahmadov G., Sadigov A.,

Suleymanov S., Zerrouk F. //Journal of Instrumentation, -2017,Vol. 12, №2, -p.1-7.
11. Ahmadov F., New phoswich detector based on LFS and p-terphenyl scintillators coupled to Micro Pixel Avalanche Photodiode / Abdullayev F, Ahmadov G, Sadigov .A, Sadygov Z, Suleymanov S, //Functional Materials, -2017, Vol.24, No.2, -p.341-344.
12. Ahmadov F, On iterative model of performance of micropixel avalanche photodiodes / Abdullayev F, Akberov R, Ahmadov G, Sadygov Z Sadigov, A., Suleymanov S // Nuclear Instruments and Methods in Physics Research Section A: Accelerators, Spectrometers, Detectors and Associated Equipment,-2018, A912, -p.287-289 .
13. Akbarov R, Scintillation light detection with MAPD-3NK and MPPC-S12572-010P readout/ Ahmadov F, Ahmadov G, Sadygov Z, Sadigov A, Suleymanov S// KnE Energy & Physics DOI: 10.18502/ken.v3i1.1767
14. Ahmadov F., A new physical model of Geiger-mode avalanche photodiodes/ Abdullayev F, Ahmadov G, Sadigov .A, Sadygov Z, Suleymanov S // Journal of Instrumentation, -2020, Vol 15, -p. 1-8.
15. Holik M, Miniaturized read-out interface "Spectrig MAPD" dedicated for silicon photomultipliers/ Ahmadov F, Ahmadov G, Akbarov R, Berikov D, Mora Y, Nuruyev S, Pridal P, Sadygov A, Sadygov Z, Zich J// Nuclear Instruments and Methods in Physics Research Section A: Accelerators, Spectrometers, Detectors and Associated Equipment,-2020, A978, -p. 1-9.
16. Ahmadov F.,Ahmadov G., Sadigov A.,Sadygov Z., Suleymanov S., R.Madatov, New phoswich detector based on MAPD and LFS & P-terphenyl scintillator //Fifth International Conference "Engineering of Scintillation Materials and Radiation Technologies" , -Minsk, Belarus:-26 - 30 September, -2016,- p 13.
17. Ahmadov F., Ahmadov G., Garibov A., Madatov R., Naghiyev J., Olshevski A., Sadigov A., Sadygov Z., Suleymanov S., Zerrouk F., Study on possibilities of establishing radiation

dosimeters based on silicon micro-pixel avalanche photodiode//The Third International Conference on Radiation and Applications in Various Fields of Research (RAD 2015), -Montonegro: -2015, -p. 383-385.
18. Ahmadov F.,Ahmadov G., Guliyev E., Sadigov A.,Sadygov Z., Suleymanov S., Zerrouk F., New gamma detector module based on new model micro-pixel avalanche photodiode //IWORID-2016, -Spain: -2016, -p.78.
19. S. Nuriyev, Ahmadov F., Ahmadov G., Sadygov Z., Sadigov A., Suleymanov S., Performance of the New Generation of Micropixel Avalanche Photodiodes with High Pixel Density and Photon Detection Efficiency //8th International Conference on New Developments in Photodetection, -Tours, France: -2-8 July, -2017, -p.167.
20. Ahmadov F, Sadigov A., Ahmadov G., Sadygov Z., Abdullayev F., A new physical model of the performance of avalanche photodiodes with single photoelectron detection// International Conference on the Advancement of Silicon Photomultipliers, -Schwetzingen, Germany:-11-15 June, -2018,-p.1
21. Ахмедов Ф.И., Ахмедов Г.С., Садыгов А.З, Аббасов .И.И, Квантовая Эффективность двух структур лавинных фотодиодов//11-я Международная конференция ЯДЕРНАЯ И РАДИАЦИОННАЯ ФИЗИКА, -Астана, Казахстан: -12-15 Сентябрь, -2017, -с. 179.
22. M. Holik, F. Ahmadov, G. Ahmadov, R. Akbarov, D. Berikov, Y. Mora, S. Nuruyev, P. Pridal, A. Sadygov, Z. Sadygov, J. Zich, The miniaturized read-out interface “SPECTRIG MAPD” dedicated for silicon photomultipliers//12th International ”Hiroshima” Symposium on the Development and Application of Semiconductor Tracking Detectors (HSTD12), -Hiroshima, Japan: -Dec 15-18,- 2019, -p.1.

The defense will be held on «15» June 2021- at «15⁰⁰» a.m. at meeting of the Dissertation Council BED 1.21 of Supreme Attestation Commission under the President of the Republic of Azerbaijan operating at the Institute of Radiation Problems

Address: AZ 1143, Baku, st. Vahabzade, 9

Dissertation is accessible at the library of the Institute of Radiation Problems of the National Academy of Sciences of Azerbaijan.

Electronic versions of dissertation and its abstract are available on the official website of the Institute of Radiation Problems of ANAS

Abstract was sent to the required addresses on «24» May 2021

Signed for print: 22.05.2021
Paper format: _60x84, 1/16__
Volume: __78860__characters
Number of hard copies: __20____